Załącznik nr 3 w postępowaniu habilitacyjnym – Autoreferat w wersji angielskiej

Summary of professional achievements

Michał Nowak

AGH University of Science and Technology
Academic Centre for Materials and Nanotechnology

Krakow, March 28, 2019

To my wife Magdalena,
whose dedication and support made this work possible.

Contents

1. Personal data

Name and surname: Michał Nowak
Current employment: AGH University of Science and Technology,
Academic Centre for Materials and Nanotechnology
Phone: (+48) 12 617 20 73
e-mail: mpnowak@agh.edu.pl
www: mpnowak.org

2. Diplomas and scientific degrees

1. **Master of Science in technical physics**, 26.06.2008. AGH University of Science and Technology, Faculty of Physics and Applied Computer Science. Master thesis title: *Molecular coupling for electron pair in a stack of self-organized quantum dots*, thesis supervisor prof. dr hab. inż. Bartłomiej Szafran.

2. **Ph. D. in physics**, 28.10.2013. AGH University of Science and Technology, Faculty of Physics and Applied Computer Science and University of Antwerp – Ph. D. diploma of both universities. Ph. D. thesis title: *Electronic structure of artificial atoms and molecules: spin-orbit coupling effects*. Thesis supervisors: prof. dr hab. inż. Bartłomiej Szafran, prof. Francois Peeters. Diploma with honors.

3. Employment in scientific institutions

1. 10.2013 – 09.2017, assistant at the Faculty of Physics and Applied Computer Science, AGH University of Science and Technology, Poland.

2. 01.2015 – 12.2016, Postdoctoral researcher, QuTech and Kavli Institute of Nanoscience, Delft University of Technology, Delft, The Netherlands.

3. 10.2017 – until now, assistant professor at Academic Centre for Materials and Nanotechnology, AGH University of Science and Technology, Poland

4. Scientific achievement, following the law on scientific degrees

As a scientific achievement, being the base of the current application, I present a series of articles on a common topic.

4.1. Title of the achievement

Spin effects and induced superconductivity in semiconducting nanostructures

4.2. Authors, titles of publications, publication year, publisher

[H1] **M. P. Nowak**, B. Szafran, *"Spin current source based on a quantum point contact with local spin-orbit interaction"*, Applied Physics Letters 103, 202404 (2013). [IF 3,5]

[H2] **M. P. Nowak**, K. Kolasiński, B. Szafran, *"Signatures of spin-orbit coupling in scanning gate conductance images of electron flow from quantum point contacts"*, Physical Review B 90, 035301 (2014). [IF 3,7]

[H3] **M. P. Nowak**, B. Szafran, *"Single-electron shell occupation and effective g-factor in few-electron nanowire quantum dots"*, Physical Review B 91, 085102 (2015). [IF 3,7]

[H4] M. Kjaergaard, F. Nichele, H. J. Suominen, **M. P. Nowak**, M. Wimmer, A. R. Akhmerov, J. A. Folk, K. Flensberg, J. Shabani, C. J. Palmstrøm, C. M. Marcus, *"Quantized conductance doubling and hard gap in a two-dimensional semiconductor-superconductor heterostructure"*, Nature Communications 7, 12841 (2016). [IF 12,1]

[H5] M. Kjaergaard, H. J. Suominen, **M. P. Nowak**, A. R. Akhmerov, J. Shabani, C. J. Palmstrøm, F. Nichele, C. M. Marcus, *"Transparent Semiconductor-Superconductor Interface and Induced Gap in an Epitaxial Heterostructure Josephson Junction"*, Physical Review Applied 7, 034029 (2017). [IF 4,8]

[H6] J. Kammhuber, M. C. Cassidy, F. Pei, **M. P. Nowak**, A. Vuik, Ö. Gül, D. Car, S. R. Plissard, E. P. A. M. Bakkers, M. Wimmer, L. P. Kouwenhoven, *"Conductance through a helical state in an InSb nanowire"*, Nature Communications 8, 478 (2017). [IF 12,4]

[H7] H. Zhang, Ö. Gül, S. Conesa-Boj, **M. P. Nowak**, M. Wimmer, K. Zuo, V. Mourik, F. K. de Vries, J. van Veen, M. W. A. de Moor, J. D. S. Bommer, D. J. van Woerkom, D. Car, S. R. Plissard, E. P. A. M. Bakkers, M. Quintero-Pérez, M. C. Cassidy, S. Koelling, S. Goswami, K. Watanabe, T. Taniguchi, L. P. Kouwenhoven, *"Ballistic superconductivity in semiconductor nanowires"*, Nature Communications 8, 16025 (2017). [IF 12,4]

[H8] **M. P. Nowak**, P. Wójcik, *"Renormalization of the Majorana bound state decay length in a perpendicular magnetic field"*, Physical Review B 97, 045419 (2018). [IF* 3.8]

[H9] P. Wójcik, **M. P. Nowak**, *"Durability of the superconducting gap in Majorana nanowires under orbital effects of a magnetic field"*, Physical Review B 97, 235445 (2018). [IF* 3.8]

[H10] **M. P. Nowak**, P. Wójcik, *"Probing Andreev reflection reach in semiconductor-superconductor hybrids by Aharonov-Bohm effect"*, Applied Physics Letters 114, 043104 (2019). [IF* 3,5]

[**H11**] **M. P. Nowak**, M. Wimmer, A. R. Akhmerov, *"Supercurrent carried by non-equlibrium quasiparticles in a multiterminal Josephson junction"*, Physical Review B 99, 075416 (2019). [IF* 3.8]

The values of Impact Factor (IF) coefficients are given after the Journal Citation Reports base, according to the year of publication or (*) with the latest available value.

The co-authors' statements regarding their contribution to the above -mentioned publications can be found in **attachment no 5**: *co-authors' statements.*

4.3. Description of the aim of the articles listed above and the results obtained as well as their possible application

Introduction

My scientific work which is the subject of this application and which was my area of interest in the recent years focuses on the theoretical description of spin effects and induced superconductivity in semiconductor nanostructures, in particular in the context of the use of these phenomena for engineering of topological superconductivity.

Semiconductor nanostructures are electronic components whose dimensions are tens or hundreds of nanometers. Due to their size, they allow investigating and controlling of individual charge carriers. This led to demonstration of the fundamental phenomena resulting from the quantum nature of the world on the nano scale such as quantization of conductivity in quantum point contacts (QPCs) [1] or appearance of discrete energy spectra of artificial atoms and molecules [2]. Since the end of the twentieth century, intensive research has been carried out on the spin properties of nanostructures. Of particular interest is the possibility of using these systems to build elements of the new electronics that exploits the additional degree of freedom [3] and an application of nanostructures to build quantum computer components using spin as a carrier of quantum information [4]. So far, the operation of the basic elements of a quantum computer based on the electronic spin [5] has been successfully demonstrated. However, the practical implementation of the scalable structures still remains a problem, due to the fast decoherence of qubits resulting from their interaction with the environment, in particular nuclear spins.

At the same time, a novel branch of research began to gather considerable interest – the topological phases of matter (which finally was the subject of the Nobel Prize in 2016). A particularly interesting type of this state is topological superconductivity. It has been shown that in the systems implementing this phase – realizing triplet type superconductivity (p pairing) – on defects peculiar states are created: Majorana bound states. These quasiparticulate excitations correspond to Majorana fermions – spin-free, zero-charge, zero-energy particles that are their own antiparticles. They were already predicted in the 30's and until now were unsuccessfully sought among elementary particles. Their emergent quasi-particle implementation can be used to store quantum information in a way that avoids the problem of decoherence [6]. However, the obstacle to their experimental implementation was the fact that bulk materials that allow the implementation of topological superconductivity are in principle currently not available.

Only ten years ago, it was realized that the topological superconductor can be created artificially – by utilization of a hybrid system in which low-dimensional semiconductor nanostructures are connected to the mesoscopic s superconductor [7, 8]. Importantly, spin phenomena in nanostructures play a key role in the implementation of such a phase. To illustrate the engineering of such a phase, let us consider

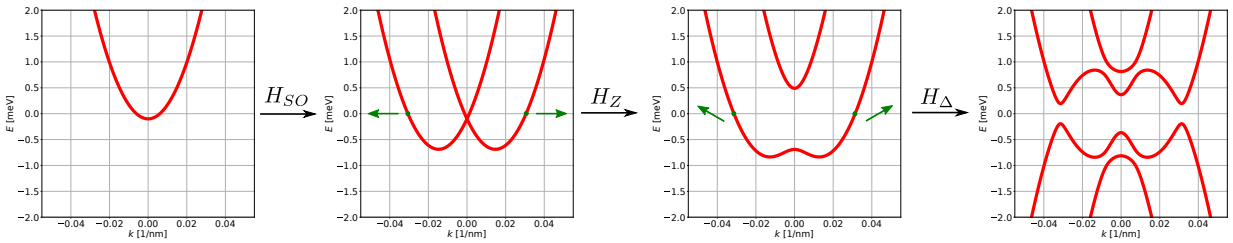

Figure 1: The evolution of the dispersion relation of a one-dimensional wire described by Hamiltonian (1) due to the inclusion of its individual elements: a single parabola splits into two bands with opposite spin polarizations after the addition of SO interaction (H_{SO}); then the Zeeman coupling (H_Z) opens the helical gap by binding the expected spin value (green arrow) with the propagation direction for zero energy states; ultimately, superconducting pairing (H_Δ) couples the electron and hole bands creating a topological gap at zero energy. For this range of parameters, the degenerate Majorana states being a mixture of electrons and holes with opposite spin polarizations will arise at the ends of a closed system.

a system described by the Hamiltonian in the form of:

$$H = \left(\frac{\mathbf{p}^2}{2m^*} - \mu\right)\sigma_0\tau_z + H_{SO}\tau_z + H_Z\tau_0 + H_\Delta\tau_x, \tag{1}$$

acting on the wave function $\Psi = (\psi_e^\uparrow, \psi_e^\downarrow, \psi_h^\downarrow, -\psi_h^\uparrow)^{\mathrm{T}}$, where σ_i (τ_i) are Pauli matrices acting on spin (electron-hole) degree of freedom. In addition to the kinetic part in Hamiltonian there are three key components:

- Spin-orbit (SO) interaction which is a relativistic effect in which an electrically charged particle propagating with the $\mathbf{k}$ momentum in an external electric field $\mathbf{E}$ experiences an effective magnetic field $\mathbf{B_{SO}} = (-1/m_0c)\mathbf{k}\times\mathbf{E}$. In crystalline materials, we deal with electric fields resulting from internal (crystalline) inversion symmetry or structure inversion symmetry breaking, which leads to Dresselhaus [9] and Rashba [10] couplings, respectively. Particularly in quasi-one-dimensional nanowires [111] with zinc blende structure there is only Rashba interaction with the Hamiltonian $H_{SO} = -\alpha k_x\sigma_y$, which causes split of the one-dimensional wire dispersion relation in the k space shown on the second panel of Fig. 1.

- Zeeman interaction, coupling the spin of charge carriers with an external magnetic field, alligned noncollinear with the direction determined by the interaction SO ($\mathbf{B_{SO}}$) with the Hamiltonian $H_Z = \frac{1}{2}g\mu_B B\sigma_{z(x)}$. It breaks the time-reversal symmetry, and together with SO interaction binds the charge carrier spin with its momentum opening the helical gap in the spectrum – see the third panel Fig. 1.

- Superconducting pairing potential included through the Hamiltonian $H_\Delta = \Delta\sigma_0$, which couples electron with its antiparticle – hole. In experimental structures this pairing results from proximitizing the semiconductor nanostructure with a superconductor. As a result of the spin interactions, the pairing potential leads to coupling of the electron band and holes with opposite spin polarizations[1] opening the topological gap at the Fermi level – see the last panel Fig. 1.

The combination of spin interactions allows for the creation of an effectively spinless state (the spin state is determined by momentum), which after inducing superconductivity realizes the effective

[1]Each time we mention *spin polarization* in a quasi-one-dimensional systems or under the simultaneous presence of SO and Zeeman interactions, we mean polarization to an approximate degree.

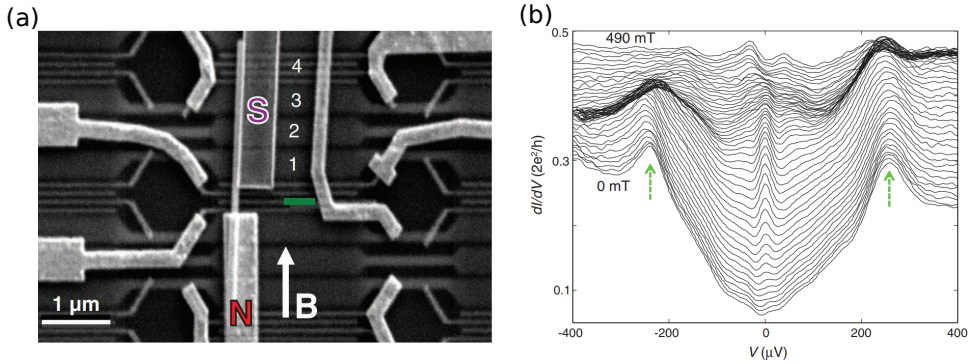

Figure 2: (a) Hybrid structure in which the first measurement of Majorana bound states was made: a semiconductor nanowire covered by a metal (N) and a superconducting (S) electrode on top of a series of transverse electrodes generating potential barriers and locally controlling the chemical potential in the structure under the presence of an external magnetic field (B). (b) Tunnel spectroscopy of the structure with visible coherence peaks (green arrows) showing the induced superconducting gap in the nanowire and the formation of zero energy peaks corresponding to Majorana states in a non-zero magnetic field. The drawings are from work [11].

phase of topological superconductivity. The Majorana states are then formed at the edges of the system [7, 8]. Immediately after this theoretical predictions were published the race began in an experimental demonstration of the presence of Majorana states, and thus the creation of the topological superconductivity phase. In 2012, a group from Delft (Prof. Leo Kouwenhoven), was the first to demonstrate measurements of tunnel spectroscopy of a nanowire proximitized by a superconducting gate showing the presence of Majorana bound states [11] – see Fig. 2. Soon similar observation were reported by other groups [12–15] and it seemed that the implementation of more complex devices capable of using Majorana bound states to implement protected topological quantum computing is only a matter of the next few years.

Research aim

During the following years after the original experiment in Delft, as the work on hybrid nanodevices has progressed, it was realized that these systems are extremely complex and have rich physics. This is mainly due to the fact that these nanostructures combine materials of a distinctly different nature – a metallic superconductor in which electrons exist as a Cooper pair condensate with a semiconductor in which spin phenomena dominate.

In the years when the first measurements of Majorana states were made, both repeatable methods of producing such systems were lacking, and the structures themselves were of low quality. This raised questions whether the measurements of the first experiments are unambiguous. Among other things, there were arguments that tunnel spectroscopy measurements are not a reliable determinant of the presence of boundary states – the result of spectroscopic measurements can be caused by disorder in the system – or that so far there were no measurements indicating that a helical state is implemented in open nanowire systems.

Progress was also inhibited due to the fact that theoretical predictions based on simple models, neglecting the effects of finite transverse dimensions of quasi-1D systems, the impact of a combination of semiconductor and superconducting materials or aspects of the magnetic field such as orbital effects.

Therefore, parallel progress in fabrication of devices along with developing theoretical understanding of hybrid nanostructures become crucial for further progress in reliable engineering of topological

superconductivity in hybrid nanosctructures. My work was devoted to these studies, in which three basic goals can be distinguished:

- Investigation of the influence of SO interaction on the spin polarization of electronic states and current flowing through open structures and the possibility of quantification of this interaction.
- Explaining the influence of proximity effect on transport properties and induced superconductivity in semiconductor nanostructures.
- Investigation of the influence of orbital effects of the external magnetic field on the induced superconductivity and Majorana bound states.

Methods

My research work is based on the theoretical calculation of an electronic structure or electron transport. The methods used in the works included in the habilitation achievement can be grouped according to the nature of the phenomenon under study:

- **Methods for calculating the electronic structure**. I used the method of exact diagonalization, where the Hamiltonian of the system is discretized on the computational grid **[H8][H9]**. In the case of multi-electron systems, an exact approach (in numerical way) taking into account the electron interaction – the configuration interaction method was applied **[H3]**. These methods were implemented directly by me, without the use of external calculation codes.
- **Methods for calculating conductance**. Electron transport was described in a stationary approach by the solution of the time-independent Schrödinger equation. The considered systems were divided into a scattering region, to which semi-infinite contacts were connected. Discretized Schrödinger equation with open boundary conditions in the contacts led to a system of equations whose solution allowed to determine the scattering matrix. Then, in the Landauer-Büttiker approach, the differential conductance of the system was determined. This method was explicitly implemented by me and those calculation codes were used in the works **[H1][H2]**. Then for the calculation in the works **[H4][H6][H7][H10]** I used the implementation of the mentioned method in Kwant package to which development I contributed during my stay in Delft.
- **Methods for calculating the current flowing through the Josephson junction**. The dissipative current flowing through the Josephson junction under applied bias voltage was calculated in the approach [16] basing on wave-function matching that accounts for quasiparticle scattering events induced by the applied voltage and Andreev reflections on the normal-supercondcutor interfaces **[H5][H11]**.

In addition, in the works presented here, I used a number of analytical methods that allowed to explain in a more detail the physical processes behind the numerical results.

In the further part of the Summary, I will discuss the most important results of the papers, according to the chronological order of their creation and the context that accompanied the research.

I began my research with a theoretical description of the impact of SO interaction on the spin properties of nanostructures, in particular those defined in open nanowires. The next four works

included in the achievement were created in cooperation with leading experimental groups during my two-year post-doctoral stay in the pioneering team of Prof. Leo Kouwenhoven in Delft. These are works in which the theory complements the experiment, enabling understanding and quantitative interpretation of the observed physical phenomena. Two of these works were done in cooperation with the group from Deft, and two with a group of Prof. Charles Marcus from Copenhagen. In all four works I am the first theoretician on the authors lists. The remaining four works are exclusively theoretical works that I did after returning to Poland (including one carried out in an international cooperation). They provide predictions regarding spin phenomena and induced superconductivity in semiconductor nanostructures, in particular in the context of the previously omitted orbital effects of the magnetic field.

Overview of the publications

[H1] M. P. Nowak, B. Szafran, *"Spin current source based on a quantum point contact with local spin-orbit interaction"*, Applied Physics Letters 103, 202404 (2013).

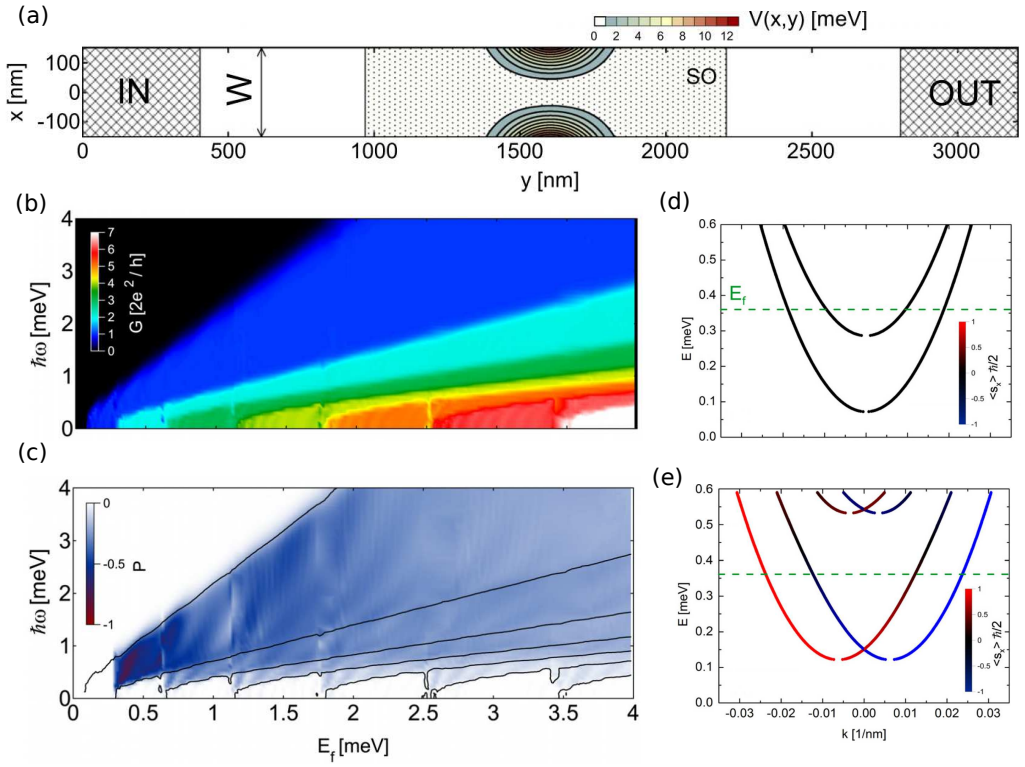

Figure 3: (a) Schematic representation of a semiconductor nanowire with local SO interaction (dotted area) with quantum point contact (colored contours) and two semi-infinite electrodes (labeled as IN, OUT). (b) Conductance map as a function of the QPC potential and Fermi energy in contacts and (c) a spin polarization map with a visible strong spin current polarization at the first quantization step of $2e^2/h$. (d) The dispersion relation in the left contact and (e) in the QPC area, the expectation value of the spin of electron propagating in the given state of transverse quantization is denoted by the color of the curve. [**H1**].

The first work is devoted to investigations of the effects of SO on the current flowing through quantum point contact (QPC) in a two-dimensional quantum wire. We considered the structure shown in Fig. 3(a), in which the SO interaction is present locally near the QPC area – which can be experimen-

tally accomplished by the presence of an additional electrode [dotted area in Fig. 3(a)]. The narrowing of the channel results in observed already in the eighties' [1] effect of conductance quantization when the narrowing of the QPC opens the transport through successive subbands of transverse quantization. However, only the progress in the fabrication of nanodevices has allowed the creation of quantum wells in materials with a strong SO interaction such as InGaAs – which is the subject of this paper.

In this work we focused on the possibility of realization of a spin-polarized current source in a quantum wire under source-drain bias. We defined the spin polarization as $P = (G_+ - G_-)/\lambda$, where $\lambda = (G_+ + G_-)$ for $G > 2e^2/h$ and $\lambda = 2$ for $G \leqslant 2e^2/h$, and $G_\pm$ defines conductance for positive and negative spin polarization of charge carriers at the output of the system. Fig. 3(b) shows the conductance map as a function of the potential generated by QPC electrodes and Fermi energy with visible steps of $2e^2/h$. Map Fig. 3(c) presents the spin polarization of the current at the output of the device. We observed that P acquires non-zero values with the highest absolute value (up to $P \simeq -0.8$) on the first quantization step i.e. when two modes propagate in the QPC.

To explain this effect, we have pointed out that for 2DEG the SO coupling Hamiltonian has a form depending on the momentum operator in both x and y directions. As a result of mixing transverse quantization states with opposite spin polarizations in the QPC constriction, for electrons propagating towards the output electrode, there are modes available whose total expected value of spin in the x direction is negative [green dotted line in Fig. 3(e)]. This causes that initially spin degenerate current acquires polarization when flowing through the narrowing due to the dominant transmission of bands in which the spin is set antiparallel to the x direction. The map Fig. 3(c) shows that the spin current polarization is obtained in a wide range of parameters – Fermi energy and narrowing potential.

The proposed effect can be used to build a fully electric source of spin polarized current in semiconductor structures. This would solve the problem of a very low degree of spin current polarization obtained by contacting a semiconductor material with ferromagnetic contacts [17].

[H2] M. P. Nowak, K. Kolasiński, B. Szafran, *"Signatures of spin-orbit coupling in scanning gate conductance images of electron flow from quantum point contacts"*, Physical Review B 90, 035301 (2014).

In the previous work, we pointed out that the SO interaction, despite inducing the spin polarization of the current, does not break Kramers degeneracy – the conductance remains quantized in multiples of $2e^2/h$. Bearing in mind the phenomenon of mixing transverse states by the SO interaction, we asked ourselves whether the effects of this coupling can be observed directly – by depicting the structure of the current flowing from the QPC. The technique that enables such imaging is the scanning gate microscopy (SGM). In this method, the charged tip of the atomic force microscope scans the surface over the heterostructure and introduces a local potential in 2DEG [18] that reflects the propagating electrons. Previously, this enabled demonstration that the current flowing from the QPC forms branches whose number corresponds to the number of transverse modes propagating through the constriction [19].

We considered a system depicted in Fig. 4 (a) that contained a QPC defined in a two-dimensional channel. The tip of the atomic force microscope scans the area behind the QPC in the same way as in experimental measurements, generating a repulsive potential island in the area of the electron gas.

In the absence of the tip, we observed the quantization of conductance as a function of the QPC potential – Fig. 4 (b) – as in the case of the previous work. The maps Fig. 5(a)-(c) show the change in conductance after the introduction of the potential of the tip (relative to the reference value obtained

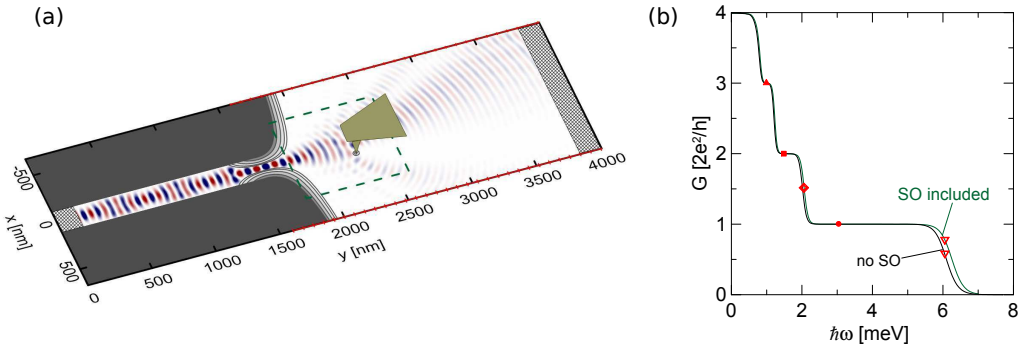

Figure 4: (a) Schematics of the considered system. Gray contours show the potential of confinement at the input contact and QPC. Above the structure there is a charged tip of atomic force microscope, which locally disturbs the potential in the electron gas changing the trajectories of propagating charge carriers. The real part of the wave function is shown in red and blue. The red color at the perimeter of the system indicates the area where open boundary conditions were applied. (b) Quantized conductance as a function of QPC potential. [**H2**].

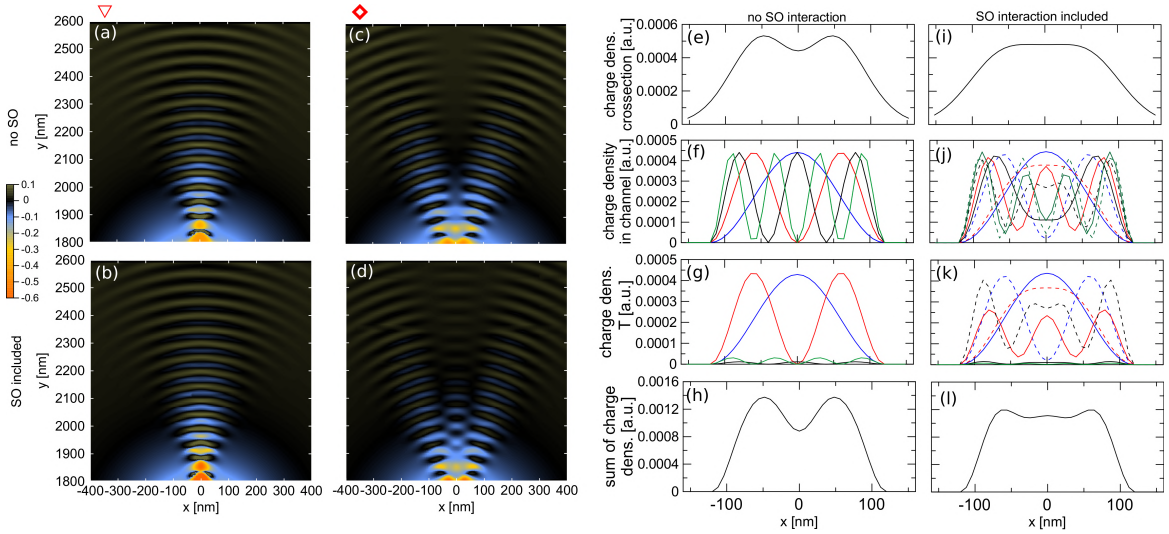

Figure 5: (a)-(d) Conductance maps obtained by scanning gate microscopy for two QPC potential values marked with a triangle and a diamond in Fig. 4 (b). (e)-(i) Cross-section of probability density in the position after the QPC. (f)-(j) The probability densities in the output channel and the densities multiplied by the probability of transmission to a given mode (g)-(k). (h)-(l) Sum of densities from panels (e)-(i). Panels (e)-(h) are obtained in the absence of SO interaction and panels (i)-(l) with SO coupling included. [**H2**].

in the absence of the tip). We observed the previously mentioned branched electron flow. The maps show the interference pattern with fringes separated by half the Fermi wavelength. The number of branches is proportional to the number of transmitted transverse quantization states in the constriction – compare Fig. 5(a) and (c). This is illustrated in more detail in Fig. 5(e), where we show the charge density cross-section just behind QPC. When the conductance of a non-perturbed system is $2 \cdot 2e^2/h$ its shape results from the ideal transmission of two modes by QPC – Fig. 5(g) – the sum of charge densities in the cross-section gives a distribution with two maxima.

After taking into account the SO interaction, we observed the appearance of an additional branch in the current flow – see the map Fig. 5(d). As demonstrated in the paper [**H1**], SO interaction in a two-dimensional systems leads to the mixing of transverse quantization states. As a result of mixing with

higher energy states – electrons in QPC populate subsequent states of transverse excitation [however, the total sum of transmission coefficients remains unchanged] – and transmission probabilities for modes are no longer binary [compare Fig. 5(g) and (h)]. Ultimately, the cross-section of the total charge density behind QPC has three maxima [Fig. 5(l)] which is reflected on the conductance map Fig. 5(d). It is worth noting that the impact of SO does not change the separation of the fringes in the conductance maps, which indicates that the back reflections from the potential of the tip are processes that do not change the spin of the charge carriers.

In addition to the main result described above, work **[H2]** demonstrates the effect of SO interaction on the conductance maps obtained for QPC potential tuned such the conductance exhibits plateaus with multiplies of conductance quanta and we discussed in detail the impact of SO coupling on the spatial distance of conductance fringes and the influence of QPC geometry on the obtained results. The phenomenon discussed in the work constitutes a new measurement method for determining the presence of SO interaction in the two-dimensional structures.

[H3] M. P. Nowak and B. Szafran, *"Single-electron shell occupation and effective g-factor in few-electron nanowire quantum dots"*, Physical Review B 91, 085102 (2015).

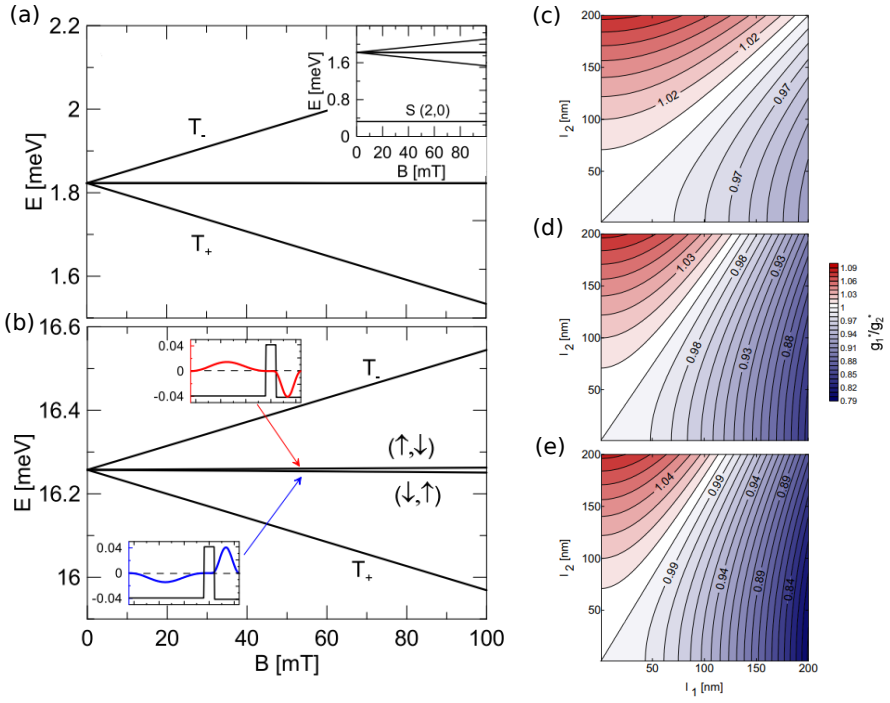

Figure 6: The spectrum of a two-electron, double quantum dot in the case when both dots have the same size (a) and when one of them is longer (b). Insets in the panel (b) show the spin density in both dots. (c)-(e) the ratio of the effective Landé factors in the first and the second dot with respect to the length of the dots for the case of: (c) two-electron, (d) four and (e) six electrons occupying the dots. **[H3]**.

The second key ingredient for inducing the topological phase is the Zeeman interaction. It has to be strong enough to open the helical gap for small magnetic fields – smaller than the critical field of the thin superconductor layer covering the semiconductor. Its dependence on the external magnetic field is determined by the Landé g-factor. At the time when the first observation of Majorana states was made, the values of the Landé factor in nanowires were known mainly from measurements of electric

dipole spin resonances (EDSR) [20], where the resonance energies determine the strength of Zeeman spin splittings. This method relies on lifting the Pauli blockade in a two-electron double quantum dot. However, some of the experiments [21, 22] studied nanodevices with more than two electrons, assuming that such an arrangement is the equivalent of a two-electron system. Work **[H3]** verifies this assumption and explains the effect of occupation of the dots on the obtained g-factor values.

We considered a system of coupled quantum dots defined in a quasi-one-dimensional quantum wire. Using a numerically exact configuration interaction method we described $2N$ interacting electrons. We considered the voltage configuration on the electrodes that tune the chemical potential in the dots such Pauli blockade is realized – the ground state of the system is the singlet state. Then the electrons occupy one of the dots [see inset in Fig. 6(a)] blocking the electron transport through the system. We showed that in a two-electron system, when the dots are of different sizes, the degeneracy between the singlet states (S) and triplet states (T_0) [for the symmetrical layout shown in Fig. 6(a)] is lifted – the effective g-factor is different in the two dots – what results in the appearance of states in which spin polarization in the dots is opposite [see Fig. 6(b)]. It should be noted that the latter effect is solely induced by the presence of SO interaction and not the variation of the Landé factor due to changes in material parameters. We also showed that in the case of the dots occupied by more electrons, this effect occurs even for a symmetrical system due to the filling of the dots with different amounts of electrons. In the paper, we gave analytical estimates of ratio of effective g-factor in the two dots – with the values presented in Fig. 6(c)(d)(e) and we showed that the Landé factor ratio increases with increasing number of electrons, which explained the experimental observations of the time.

Finally, in the work we showed that for systems with $N > 1$ all except two electrons, form closed singlet shells. Nevertheless, such systems can not be treated as the equivalent of a two-electron system. This is due to the fact that two excess electrons occupy high-energy single-electron shells, which results in a change in the measured g-factor. We proposed, however, that a multi-electron problem for $N > 1$ can be described with great accuracy by a two-electron analogue with removed orbitals that are occupied by $2N - 2$ electrons. This effect can be used in following theoretical works using the configuration interaction approach for these systems.

[H4] M. Kjaergaard, F. Nichele, H. J. Suominen, **M. P. Nowak**, M. Wimmer, A. R. Akhmerov, J. A. Folk, K. Flensberg, J. Shabani, C. J. Palmstrøm, C. M. Marcus, *"Quantized conductance doubling and hard gap in a two-dimensional semiconductor-superconductor heterostructure"*, Nature Communications 7, 12841 (2016).

In the years 2015-2016, parallel studies were carried out on proximitized two-dimensional (2DEG) and one-dimensional (nanowires) semiconductor nanostructures. The next four works describe the work that I did during my postdoctoral internship and concern both these lines of research.

During the first measurement of Majorana bound states, the problem with the quality of fabricated NS junctions became apparent. It was expected that in the proximitized semiconductor there should be no states in the induced gap – as it is the case for bulk superconductor. However the tunneling spectroscopy measurements indicated significant conductance in the superconducting gap (soft gap problem) which was speculated to be the result of disordered interface between semiconductor and superconductor. The work reports on overcoming this problem, which is reflected in two effects: a significant reduction of the conductance in the superconducting gap in the tunneling regime and the amplification of conductance by the Andreev reflection in the open regime [23].

This work was done in collaboration with the experimental group of Prof. Charles Marcus from

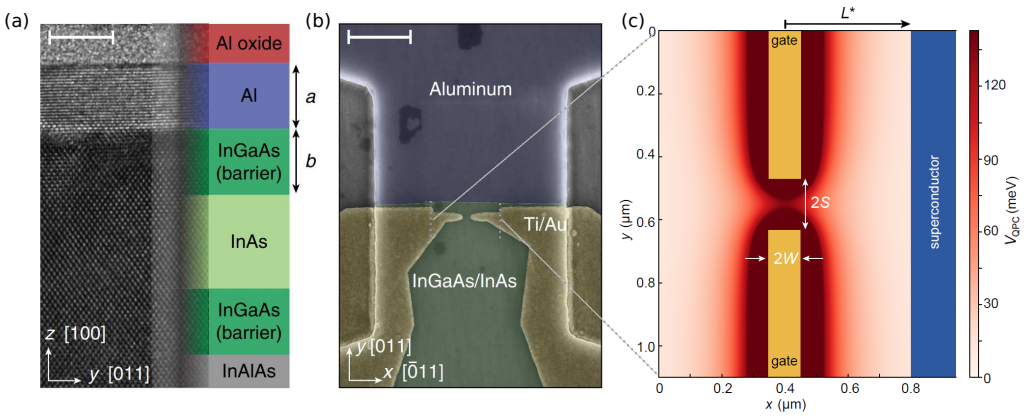

Figure 7: (a) Cross-section through the heterostructure pictured by transmission electron microscopy with the material composition denoted. The scale bar is 5 nm. (b) Experimentally measured structure depicted by scanning electron microscopy. The Ti/Au electrodes form the QPC potential in the electron gas before the proximitized part that forms a NS junction. The scale bar has 1μ m. (c) Structure considered in numerical simulations with the potential distribution resulting from the presence of QPC electrodes. The superconducting region is located in a distance L^* from the center of the QPC. [**H4**].

Copenhagen. We examined a semiconductor-superconductor hybrid defined on a two-dimensional electron gas in which the superconducting layer was deposited at the stage of the epitaxial growth of the structure. The experimentally measured structure is shown in Fig. 7(b) where with yellow color we mark the metal electrodes defining the QPC potential in 2DEG trapped in InAs [see Fig. 7(a)], the rest of the device was covered with superconductor (blue area) forming a semiconductor-superconductor interface behind the QPC. This system allows both tunnel spectroscopy measurements – for significantly limited QPC transmission and measurements in the open regime – for the weak potential generated by QPC electrodes. Spectroscopy curves in the open and tunnel regimes are presented with blue and red curve in Fig. 8(a) respectively. The most important result was the measurement of a significant increase in conductance at $V_{sd} = 0$ in the open regime and almost zero conductance in the gap in the tunneling regime.

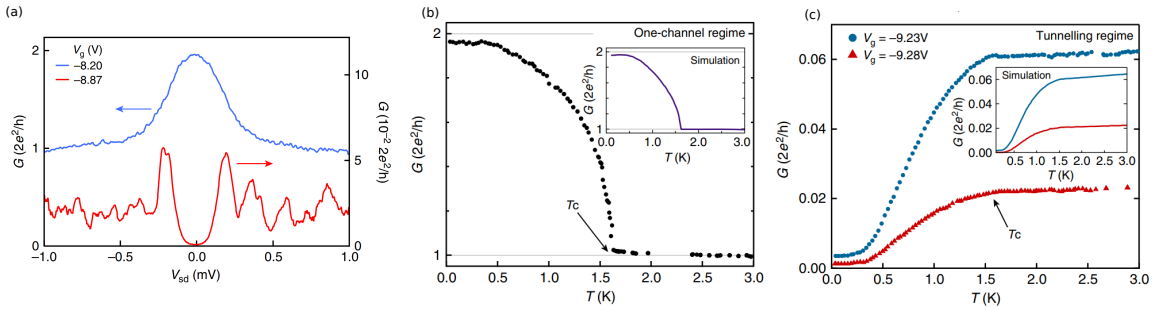

Figure 8: (a) Experimentally measured conductance in the open (blue curve) and tunnel (red curve) regimes. (b)-(c) Experimentally measured dependences of conductance at zero bias voltage relative to temperature. The insets show the curves obtained in the simulation for the geometry of the system presented in Fig. 7(c). [**H4**].

Experimental measurements in this work are explained on the basis of realistic simulations of quantum transport. To this end, we considered the model structure of the geometry shown in Fig. 7(c) with a realistic disorder description that allowed using the previous mean free path measurements to model the potential distribution in the system [24]. We have extended approach that previously was

exploited to determine transport properties for zero Fermi energy [23], so that it would be applicable for calculation of the tunnel spectroscopy curves for varied source-drain voltages. We then used this method to determine the temperature-dependent conductance.

We performed simulations using realistic parameters of the considered system taking into account the temperature dependence of both the superconducting gap and Fermi distribution in the contacts. We found a good agreement with the experimental curves – see the comparison of the experiment and calculations in Fig. 8(b)(c). We explained that the doubling of the conductance in the superconducting gap indicates that Andreev reflection is the dominant transport mechanism through the QPC.

[H5] M. Kjaergaard, H. J. Suominen, **M. P. Nowak**, A. R. Akhmerov, J. Shabani, C. J. Palmstrøm, F. Nichele, C. M. Marcus, *"Transparent Semiconductor-Superconductor Interface and Induced Gap in an Epitaxial Heterostructure Josephson Junction"*, Physical Review Applied 7, 034029 (2017).

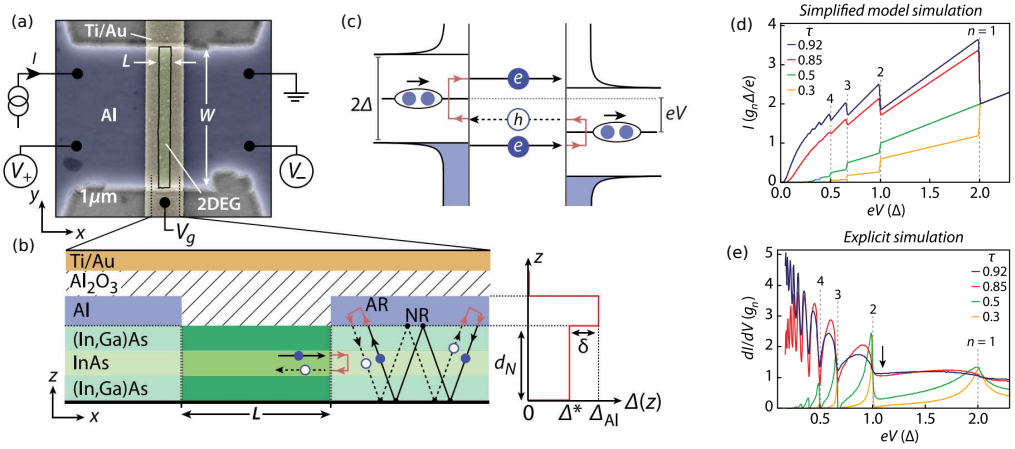

Figure 9: (a) Experimentally measured Josephson junction depicted by the scanning electron microscopy. The heterostructure is covered epitaxially with aluminum outside the narrow area marked with green color forming a S-2DEG-S junction. (b) Schematic cross-section through heterostructure with a visible electron (blue circle) and a hole (white circle) Andreev-reflecting on the interface with the area covered with aluminum. Coupling 2DEG with aluminum leads to the opening of the superconducting gap in the area marked with a light green color. (c) The schematic of the multiple Andreev reflection process. (d) The current-voltage characteristic obtained in the empirical model. (e) Conductance as a function of the source-drain voltage obtained in the exact model for several values of the transparencies of the interface. **[H5]**.

In order to unambiguously determine the quality of the 2DEG-superconductor interface, a Josephson junction was realized. Its micrograph and scheme is shown in Figs. 9(a) and (b). The channel of width W was covered with aluminum, with a gap etched in its middle, defining a normal area there. It allowed to create a semiconductor-superconductor-semiconductor (SNS) junction with controlled transparency of the normal area. It was the first such a structure realized on 2DEG in the world. After applying voltage to the junction, a dissipative current (in contrast to the superconducting current induced by the phase difference in superconductors) begins to flow. Due to the difference in voltage between source-drain electrodes the propagating quasiparticles gain energy relatively to Fermi energy in the contacts and are subject to n Andreev reflections on the NS interfaces [see Fig. 9 (c)]. As a result $(n+1)e$ charges are transfered transmitting $n/2$ Cooper pairs between superconductors. For the decreasing voltage difference, the number of Andreev reflections increases, and the resulting current

can be approximated as $I(V) \sim e(n+1)\tau^{n+1}V$, where τ is the transparency of the normal region (transmission probability of a single charge carrier). The resulting I/V trace changes its character depending on the transparency of the scattering region – see Fig. 9(d). This phenomenon was used for quantitative analysis of the properties of the measured junction. A method that accounted for coherent electron transport [16] via the SNS junction was developed which allowed to accurately determine the current and conductance of the junction [see Fig. 9(e)] for a single mode of transverse quantization. Next a model to describe the realistic, multimode, junction was proposed in which we described the current as carried by N propagating modes that belong to M subbands. Finally, the total conductance was determined as $G(V) = \sum_i^M N_i G^{(\tau_i)}(V)$.

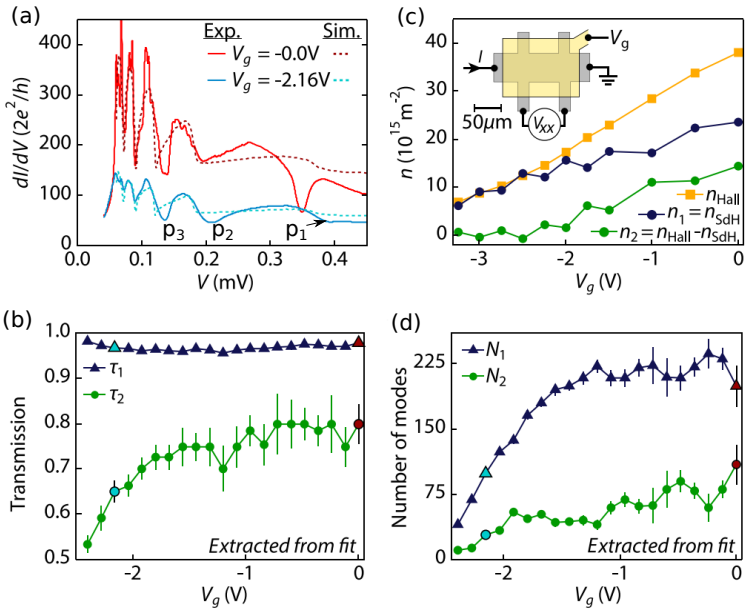

Figure 10: (a) Conductance as a function of bias voltage obtained experimentally (continuous curves) and the theoretical prediction (dashed curves) for two voltage values on the top gate. (b) Transmission probability and number (d) of modes in the two subbands. (c) Density in 2DEG obtained by magnetotransport measurement. The densities in two states of transverse quantization in the growth direction are visualized in blue and green. **[H5]**.

Figure 10(a) shows measured differential conductance curves and the theoretical predictions. We observe that for an integer fractions of the superconducting gap 2Δ local minima in the conductance curves appear – a characteristic feature of a transparent junction. It is worth noting that only the exact calculation in this work allowed for the accurate analysis of experimental curves – previously the subgap features were erroneously attributed the *maxima* curves of conductance [25–27] regardless of the junction transparency.

Fitting of the curves determined in theory to the experimental data allowed to determine the number of subbands (M), the number of modes (N_i), and the transparency of the uncovered region for each of the subbands – Fig. 10(b) and (d) respectively. Surprisingly, it turned out that the theoretical calculations clearly indicate the presence of two subbands in the system. This result became clear after additional magnetotransport measurements, which showed that in the examined heterostructure in the considered voltage ranges, we deal with electron gas occupying two states of transverse quantization in the growth direction – see Fig. 10(c).

Finally, by tracking the position of the conductance minima, we were able to determine the dependence of the superconducting gap as a function of temperature. It turned out that this relation

does not follow the BCS curve, but rather the dependency characteristic of the induced gap [28]. The analysis of the experimental results allowed to determine the parameter characterizing the quality of Al/2DEG interface as $\gamma_B = 0.87$, suggesting a pristine NS interface, which is the result of using the epitaxial process of Al deposition at the fabrication stage of the heterostructure.

The analysis of heterostructures in the above two works showed that the two-dimensional electron gas in close proximity to the superconductor is a very good base for building hybrid nanostructures with arbitrary geometry, which laid the foundations for their later use to implement the topological phase [29–32].

[H6] J. Kammhuber, M. C. Cassidy, F. Pei, **M. P. Nowak**, A. Vuik, Ö. Gül, D. Car, S. R. Plissard, E. P. A. M. Bakkers, M. Wimmer, and L. P. Kouwenhoven, *"Conductance through a helical state in an InSb nanowire"*, Nature Communications 8, 478 (2017).

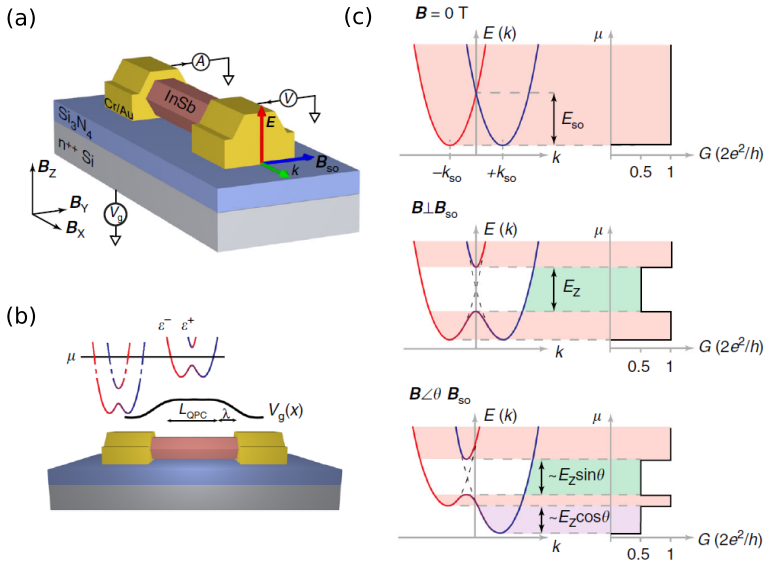

Figure 11: (a) Diagram of the experimentally measured structure with the potential profile due to the presence of the bottom gate (b). (c) The one-dimensional nanowire dispersion relations in the presence of SO interaction with the corresponding conductance curves revealing helical gap formation for the various configurations of the magnetic field. **[H6]**.

The next two papers analyze the properties of nanowires and concern the second research line in the engineering of the topological superconductivity phase.

As presented in the introduction, the prerequisite for the implementation of topological superconductivity is the creation of a helical state in a non-zero magnetic field in which electrons with opposite momenta have opposite spin polarizations. This state is reflected by the decrease in the number of subbands in the nanowire dispersion relation, and its occurrence can be confirmed by measuring the conductance – see the second panel Fig. 11(c). At the time when this study was conducted a direct demonstration of the presence of the helical state in the nanowires was missing, although measurements showing the presence of Majorana states have been available for over 4 years. This was a result of the sensitivity of the electronic transport in quasi-one-dimensional wires to disturbances and thus the inability to distinguish the effects of helical gap from resonances on the QPC potential barrier and

impurities in the system.

We proposed the use of a magnetic field with a controlled orientation with respect to the direction determined by the SO interaction to uniquely identify the helical gap in transport measurements. The idea of the experiment is presented in Fig. 11(c). We proposed that the helical gap width (E_z) should increase with the increase of the magnetic field. At the same time, we expected that by changing the alignment of the magnetic field with respect to the direction perpendicular to the axis of the wire, the width of the conductance plateau e^2/h would change and ultimately confirm the presence of the helical gap in the system.

The experiment was made on a structure shown schematically in Fig. 11(a)(b). The V_g voltage on the bottom electrode controls locally the chemical potential in the structure and creates an effective potential barrier along the nanowire.

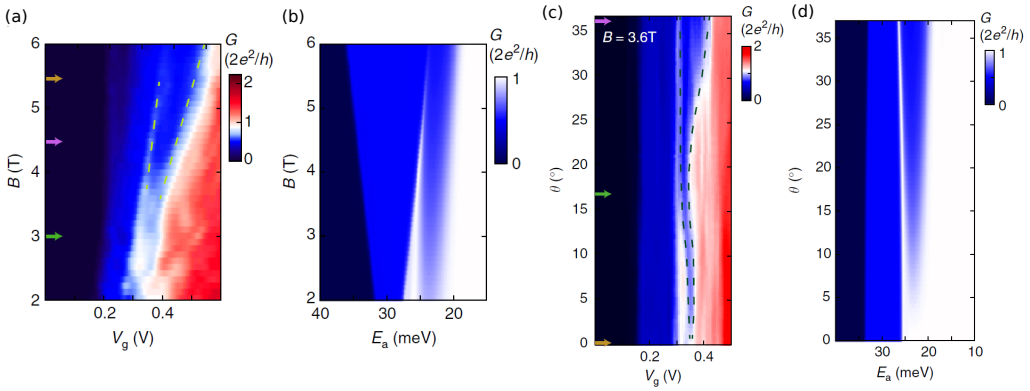

Figure 12: (a) The experimental conductance map obtained for the magnetic field set at an angle of $\theta = 17^o$ with respect to the direction of the effective magnetic field $\mathbf{B_{SO}}$. (b) Results of the numerical simulation. (c) Measurement and results of conductance modeling (d) as a function of voltage on the lower gate and the angle of the magnetic field. **[H6]**.

The experiment measured conductance of the nanowire as a function of the bottom gate voltage and the magnetic field aligned at an angle $\theta = 17^o$ with respect to the direction perpendicular to the nanowire. The result is presented in the map Fig. 12(a). In this map, a characteristic conductance pattern is visible – a peak of $2e^2/h$ surrounded by two plateau e^2/h – hallmark of the helical gap for a tilted magnetic field. Simulations conducted for the experimentally considered structure showed that indeed, for such a magnetic field orientation, the helical gap gives an image of the conductance corresponding to the measured one – see Fig. 12(b). Next the conductance measurement was made for the magnetic field of varied orientation. As mentioned above, if the conductance pattern was due to the helical gap the plateau width should vary depending on the orientation of the magnetic field [see the result of the account in Fig. 12(d)]. Such an effect was observed [Fig. 12(c)] in line with the theoretical predictions.

Importantly, the modeling allowed to estimate the SO coupling strength with the characteristic energy 6 meV. So far, the estimation of the strength of SO coupling was performed indirectly – by studying the repulsion of energy levels in quantum dots [33–35]. Here we were able to probe its value directly. Such a strong coupling measured in the considered nanowire is useful not only for the implementation of topological phases, but also allows the use of these structures as sources of spin polarized current, even in the absence of an external magnetic field, as proposed in the paper **[H1]**.

[H7] H. Zhang, Ö. Gül, S. Conesa-Boj, **M. P. Nowak**, M. Wimmer, K. Zuo, V. Mourik, F. K. de Vries, J. van Veen, M. W. A. de Moor, J. D. S. Bommer, D. J. van Woerkom, D. Car, S. R Plissard, E.P.A.M. Bakkers, M. Quintero-Pérez, M. C. Cassidy, S. Koelling, S. Goswami, K. Watanabe, T. Taniguchi, L. P. Kouwenhoven, *"Ballistic superconductivity in semiconductor nanowires."* Nature Communications 8, 16025 (2017).

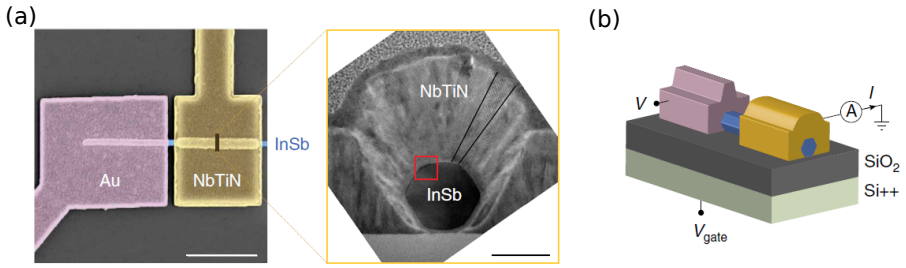

Figure 13: (a) Experimentally studied structure depicted by the means of scanning electron microscopy together with the transversal cross section revealing the InSb nanowire covered by the NbTiN superconductor layer. (b) Diagram of the measurement system – the nanowire covered with two electrodes, whose conductance is controlled by the lower gate with the applied voltage V_{gate}. **[H7]**.

Shortly after the measurements of tunnel spectroscopy presented in the seminal paper [11], it was noticed that peaks in zero energy do not definitively indicate the presence of Majorana bound states. It has been argued that at low, but finite temperature, the conductance peaks at zero energy may appear due to disorder [36–38] mimicking the signatures of Majorana states. This work studies transport in hybrid heterostructure in this context and analyzes the degree of disorder in the system. We investigated NS junction that was realized by contacting a single nanowire with a metallic and superconducting electrode, where the tunnel barrier is defined and controlled by the voltage on bottom gate [see Fig. 13(a)]. The transport measurement was performed in the configuration shown in Fig. 13(b). The measured differential conductance is presented as a function of gate voltage and source-drain voltage on the map Fig. 14(d). When the NbTiN shell is superconducting, as a result of Andreev's reflection on the NS interface, two electrons forming the Cooper pair are transmitted from the source electrode to the superconductor drain. It was expected that due to this effect the conductance at the first plateau would be doubled (as compared to the normal case) and reach the value of $4e^2/h$ [23]. The measurement, however, gave an unexpected result: despite the almost perfect quantization of the conductivity of electrons with energy exceeding the superconducting gap, the conductivity amplified by the Andreev reflection drops immediately after entering the first plateau [Fig. 14(c)].

In the normal state, the conductance is given by Landauer formula $G_n = e^2/h \sum_n T_n$, where T_n are transmission probabilities for the subsequent modes. For the conductance amplified by the Andreev reflection, at zero energy an analogous formula is given by the equation $G_s = 2e^2/h \sum_n T_n^2/(2 - T_n)^2$ (Beenakker formula) [23]). For a transport with single spin degenerate mode with $T_1 = 1$ this gives $G_n = 2e^2/h$ and $G_s = 4e^2/h$ respectively, as two charge carriers are transmitted in the superconducting regime. We have noticed, however, that if in the system there is mixing of the transverse quantization channels that leads to redistribution of the transmission probability over n modes, the Landauer formula still results in a conductance quantized in a multiples of $2e^2/h$, but the conductance given by Beenakker formula will give a result deviating from the multiples of conductance quanta to a degree proportional to the mixing ratio of the bands. To analyze this phenomenon quantitatively, simulations were carried out for the realistic geometry of the nanowire covered by the superconductor shell [see Fig.

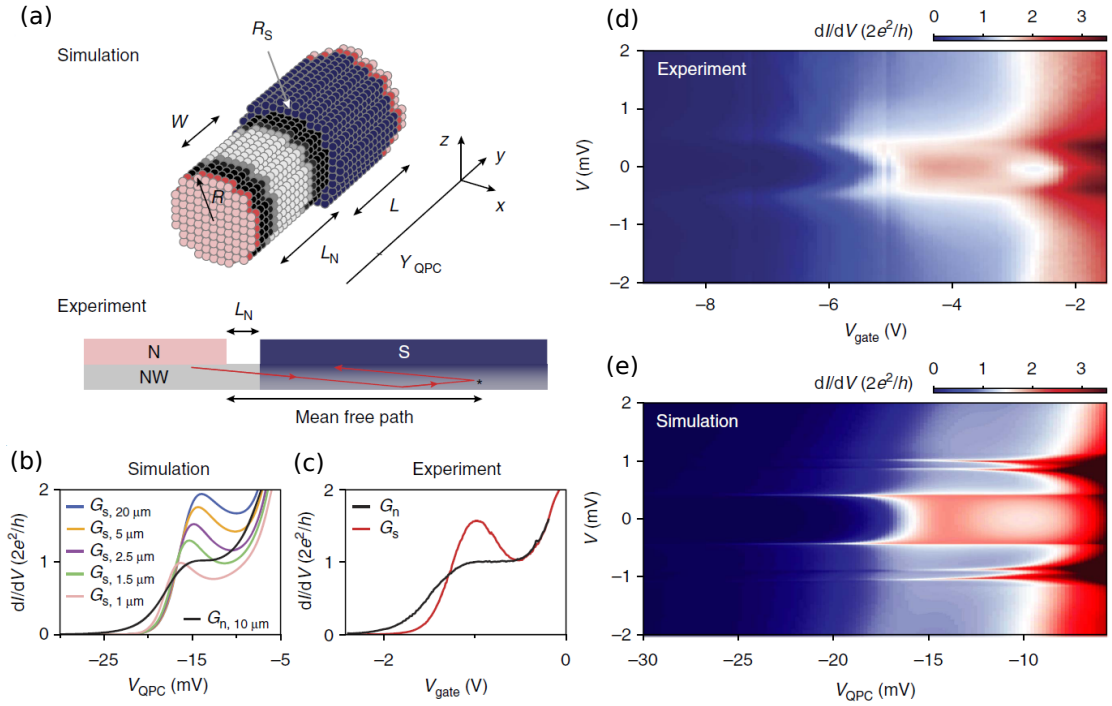

Figure 14: (a) Scheme of the modeled structure. The black color shows the nanowire with a potential barrier (gray color) covered by a superconductor (blue) with semi-infinite electrodes (pink). (b) Conductance curves obtained in simulations and (c) conductance measured in the experiment. (d) Experimental conductance map and analogous map obtained from the modeling (e). [**H7**].

14(a)]. The calculations based on solution of Bogoliubov-de Gennes equation that took into account random disorder in the semiconductor structure. We have shown that residual disorder leads to mixing of modes, without changing conductance in the normal range. In addition, even for residual disorder, the mixing of subbands is strongly amplified near the opening of the transport channel for the next subband due to the presence of van Hove singularity. Because of this, conductance amplified by the Andreev reflection has a dip as measured in the experiment [Fig. 14 (c)] – which is also apparent in measurements on 2DEG in the work [**H4**].

The non-linear dependence of G_s on T_n values allowed to determine the mean free path of the charge carriers – even if it exceeds the length of the device itself. When comparing the simulation results with experimental data, we estimated that the mean free path is of the order of micrometers, significantly exceeding the coherence length of quasiparticles in the proximitized nanowire – see Fig. 14(b). Thus, despite the lack of conductance quantization in the superconducting regime, electron transport in such a heterojunction is ballistic. The ballistic nature of proximized nanowires allows for unambiguous determination of the presence of Majorana fermions by measuring the spectroscopy of zero bias peak, which was made shortly afterwards in these wires [P19].

[**H8**] **M. P. Nowak**, P. Wójcik, *"Renormalization of the Majorana bound state decay length in a perpendicular magnetic field"*, Physical Review B 97, 045419 (2018).

One of the most fascinating applications of Majorana states is the possibility to use them for quantum computations that exploit the topological protection of *degenerate* bound states. In real systems, the Majorana bound states are not localized pointwise on the opposite edges of the nanowire,

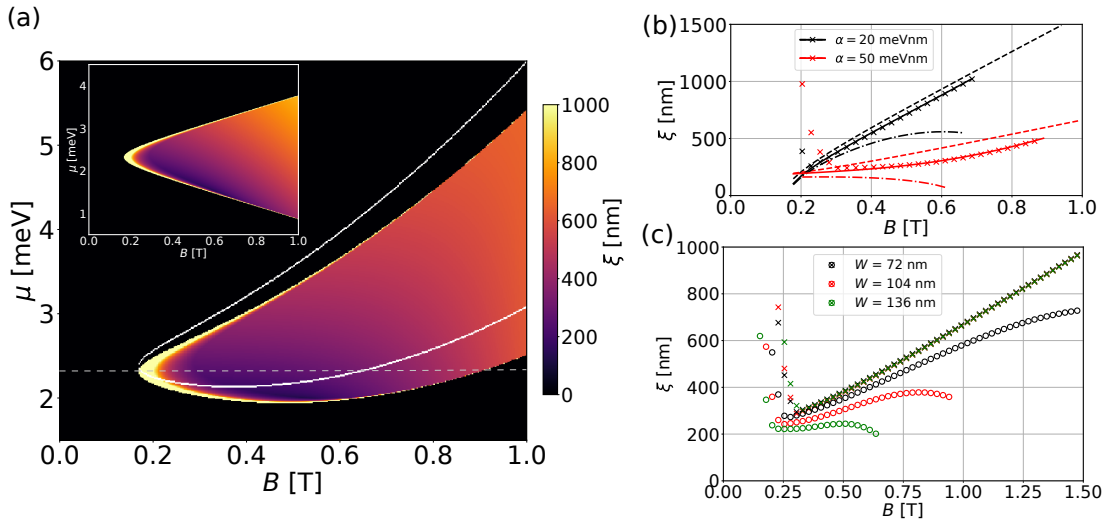

Figure 15: (a) Phase diagram as a function of the external magnetic field and chemical potential. The colors determine the coherence length of the Majorana modes (ξ). The inset shows the phase diagram when the orbital effect of the magnetic fields are neglected. (b) ξ as a function of the magnetic field obtained without orbital effects (dashed curves), with the orbital effects taken into account through the kinetic part of Hamiltonian (dotted-dashed curves) and taking full account of the orbital effects (solid curves and symbols). (c) ξ without orbital effects (crosses) and with the orbital effects included (circles) for three values of the nanowires thickness. [**H8**].

but rather gradually disappear into its interior over the length characterized by the parameter ξ. In the case when the length of the structure is comparable to ξ, the Majorana states overlap, and their energy deviates from zero and are no longer degenerate.

It was proposed that quantum computation can be accomplished by the braiding operation – by interchanging the spatial position of the Majorana states [39–41]. In this application, however, one can not use linear geometry but rather needs structures defined on nanowire crosses. Fabrication of such structures became available only recently [42–44]. However, in such systems, the magnetic field must be applied perpendicular to all nanowire branches to induce the topological phase in the whole system. The work [**H8**] describes the spatial distribution of Majorana states in the aforementioned orientation of the magnetic field.

In this work we presented an analytical model that describes the coherence length ξ in a quasi-dimensional wire, where the orbital effects of the magnetic field normalize its key parameters. These corrections can be divided into: a diamagnetic part acting as an additional chemical potential – which was noticed in a parallel work [45]; a paramagnetic part that mixes the transverse quantization modes of the nanowire; and the part resulting from the SO interaction, which mixes both the spin and the transverse excitation modes.

Figure 15(a) shows the phase diagram, where the color determines the coherence length ξ. The scaling of the chemical potential leads to a change in the shape of the topological range in the map – from the typical hyperbolic shape presented for the absence of orbital effects in the inset – to a one which is shifted in μ values for stronger magnetic field. The effects of mixing transverse excitation modes and renormalization of the chemical potential lead to a decrease in the value of ξ – see Fig. 15(b). However, we demonstrated that the impact of the SO counteracts these changes. We also performed numerical calculations for the studied nanowire and showed that shortening the coherence length of becomes significant for a wide nanowires – Fig. 15(c). The latter effect is the main message of this work: we have shown that the orbital effects of the magnetic field – so far regarded as detrimental to

the generation of Majorana bound states – can in fact stabilize zero-energy modes by decreasing the spatial span of Majorana modes.

[H9] P. Wójcik, **M. P. Nowak**, *"Durability of the superconducting gap in Majorana nanowires under orbital effects of a magnetic field"*, Physical Review B 97, 235445 (2018).

While investigating the orbital effects of the magnetic field, we realized out that previous works that considered orbital effects give contradictory information about its effect on the induced superconducting gap [46–48]. The purpose of the next work was to explain these discrepancies and propose an universal method for proper description of the orbital effects of the field for a structure with an arbitrary geometry.

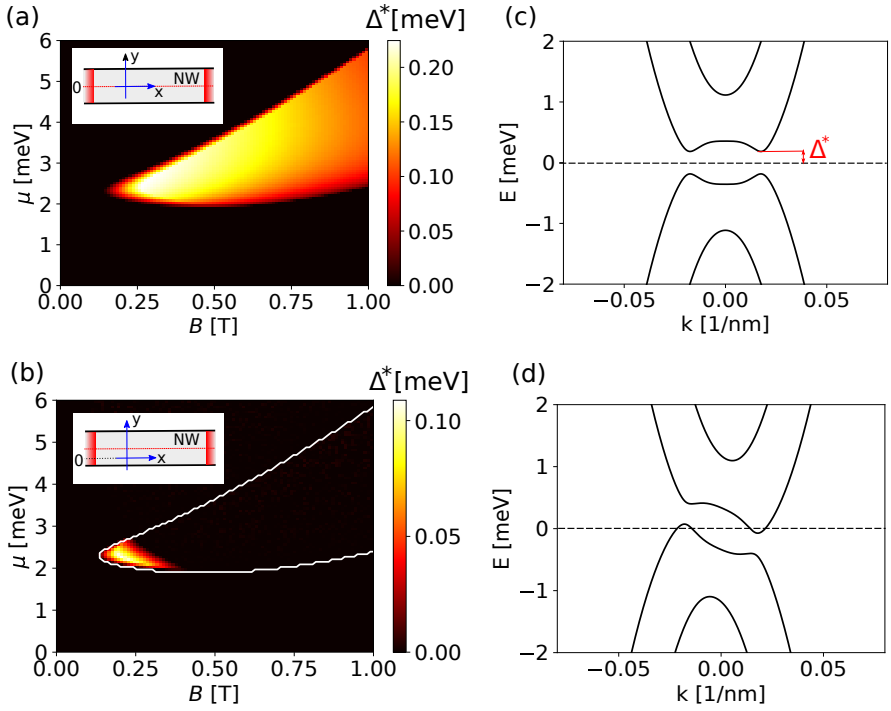

Figure 16: (a)(b) Phase diagram – the map shows the superconducting gap in the topological regime. Panel (b) presents the phase diagram for a nanowire that is located asymmetrically with respect to the center of the coordinate system. (c) The nanowire dispersion relation in the topological regime. (d) The dispersion relation with visible tilting of the bands a result of superconducting current induced in the nanowire. The dispersion relation (c) is also obtained for the system layout of (b) when the vector potential is chosen such it minimalizes the supercurrent. **[H9]**.

We considered a two-dimensional nanowire in the presence of a perpendicular magnetic field. Figure 16(a) shows the induced superconducting gap as a function of the chemical potential and the external magnetic field, for the vector potential in the form $\mathbf{A} = [-yB, 0, 0]$. By moving the nanowire relative to the coordinate system, we see that the induced gap closes already in a small magnetic field – see Fig. 16(b). It is caused by the opposite phase acquired by the electron and hole part of the wave function which results in shifting their parabolas in the dispersion relation and by that closes the induced gap at Fermi level [Fig. 16(d)]. This effect is associated with the excitation of superconducting current in the structure.

It is important to realize, that the gauge invariance guarantees that the physical properties of the

system do not change under transformation $\mathbf{A}' = \mathbf{A} + \nabla\chi$ (which is equivalent to the nanowire shift) when the pairing potential is corrected by appropriate phase factor. However the sole invariance does not determine the ground state of the system, i.e. one might choose $\mathbf{A}$ that *does* induce the supercurrent as in the case of the system Fig. 16(b) and then the invariance will preserve this supercurrent upon modification of the vector potential. In the theoretical description of hybrid nanostructures, therefore, the requirement to determine the state with the minimal supercurrent – the ground state of the system – inevitably appear. This is the key message of the described paper. Lack of such treatment led e.g. to erroneous conclusions of the work [46].

We determined a value dependent on the supercurrent – condensation energy, the minimization of which leads effectively to finding of the ground state of the system. After determining such a minimum, a non-zero superconducting gap is restored, as shown in Fig. 16 (d). An important feature of the proposed method is its universality: determining the position of the system (or vector potential) that minimizes superconducting current is often impossible a priori – in the case of spatially broken symmetries, or for more complex geometry of the system – as in the case of realistic hybrid structures.

Finally, in our work, we described the determination of the ground state for a hybrid system – a semiconductor covered with an thin aluminum layer in the strong coupling regime. We have shown that the hybridization of states in the two materials leads to the localization of charge carriers in the superconductor which results in an induced superconducting gap close to that of the superconducting material. Taking into account the orbital effects of the magnetic field and using the proposed method, we obtained critical fields corresponding to the values recently measured experimentally on gated InAs nanowires [49].

[H10] M. P. Nowak, P. Wójcik, *"Probing Andreev reflection reach in semiconductor-superconductor hybrids by Aharonov-Bohm effect"*, Applied Physics Letters 114, 043104 (2019).

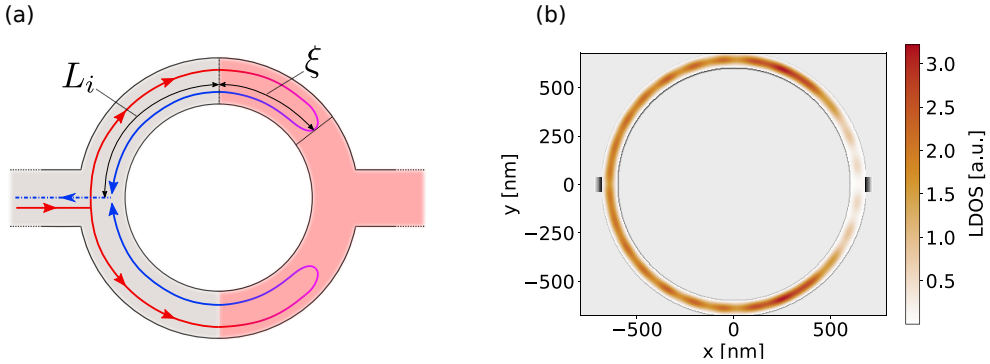

Figure 17: (a) Cartoon of the considered system: a quantum ring partially covered by a superconductor (pink area). The propagating electron (with the trajectory marked with a red curve) is Andreev reflected, penetrating the superconducting region on a distance of ξ and then returns as a hole. (b) The local density of states obtained in the transport calculations. **[H10]**.

The next work in this collection proposes to use of structures whose fabrication became possible only in recent years – hybrid quantum interferometers [44] to measure one of the key properties of hybrid nanostructures – the coherence length (ξ) over which quasiparticles with energy less than superconducting gap penetrate the proximitized semiconductor. We demonstrated how the combination of Aharonov-Bohm and Andreev reflection reveals the distance at which the electron is reflected as a hole.

We considered the system shown schematically in Fig. 17(a) – a quantum interferometer in the form of a ring partially covered by a superconductor. The electron propagating from the left electrode undergoes Adreev reflection and penetrates the superconducting region over the length of ξ in the form of an evanescent wave. Then the reflected hole returns to the left electrode. We have postulated that the phase acquired in the external magnetic field will depend both on the geometric properties of the interferometer (here L_i) and the properties of the superconductor-covered area, extending the distance at which the phase is acquired by the coherence length ξ. This length depends on the parameters of this area as $\xi = \hbar v_f/\Delta$ (where v_f is the Fermi velocity).

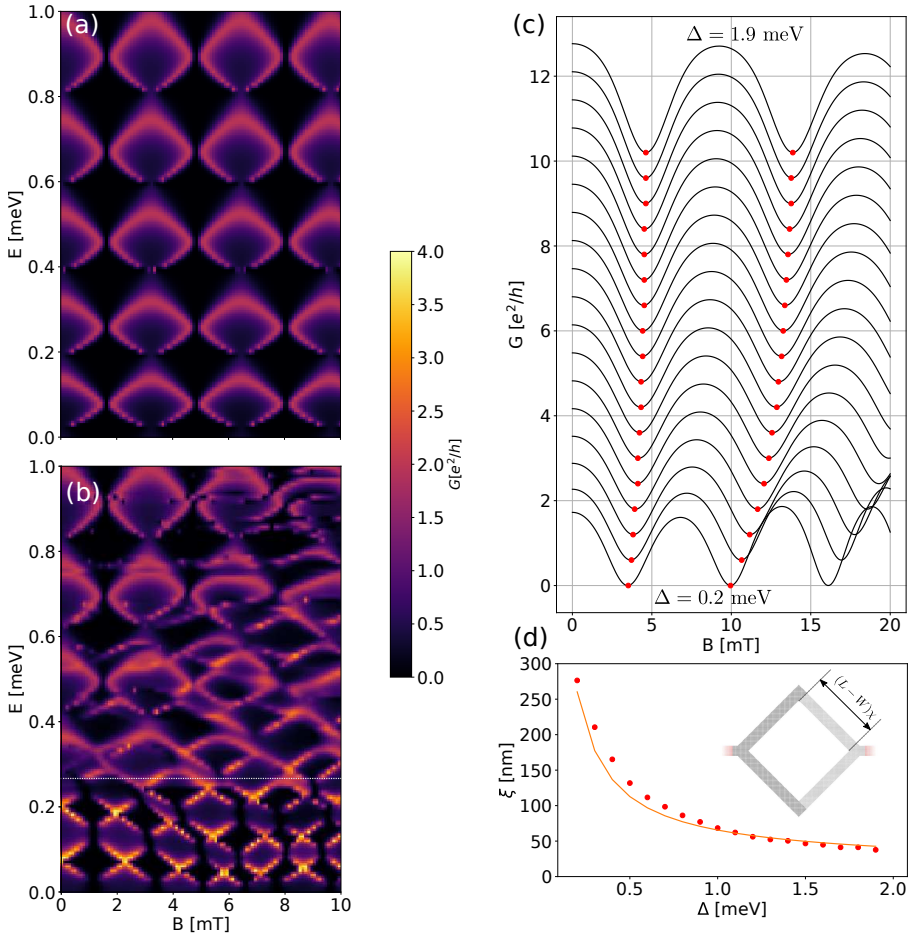

Figure 18: (a) Conductance map as a function of Fermi energy and magnetic field in the absence of induced superconductivity and (b) when it is included. (c) Conductance curves for different values of the induced gap Δ. The red dots indicate the period of Aharonov-Bohm oscillation. (d) Determined coherence length ξ for the square interferometer shown in the inset determined from the period of oscillation from the panel (c) [points] and determined directly numerically [curve]. **[H10]**.

Figure 17(b) shows the results of a numerical experiment, where we present the local density of states – vanishing density of states in the superconducting regions is visible. Maps Fig. 18(a) and (b) show conductance of the quantum ring without and with the superconductor respectively. On the panel (b) below the dotted line we can see a change in the character of the oscillation. Firstly, the maximal values of the conductance reach values $4e^2/h$ due to the transfer of two particles through the Andreev reflection process as experimentally observed in the works **[H4]** **[H7]**. Secondly we observe change of the oscillation period for the Fermi energy in the superconducting gap – in the diagram below the dotted line. When the ring is half-covered, the oscillation period is shorter than in the case

of normal ring due to the existence of an additional length on which the electron and hole propagate – ξ.

Finally, we proposed to use this phenomenon for determination the quasi-particle coherence length in currently experimentally available structures – loops fabricated from crossing nanowires – using easily achievable transport measurements. Figure 18(c) shows Aharonov-Bohm oscillations for the interferometer shown on the inset in Fig. 18(d). With the increase of the induced superconducting gap, the period of oscillation increases due to the decreasing coherence length. We determined ξ from the period of Aharonov-Bohm oscillation, observing a very good agreement with the value calculated directly by analyzing the evanescent quasiparticle modes in the proximitized channel [see Fig. 18(d)].

[H11] M. P. Nowak, M. Wimmer, A. R. Akhmerov, *"Supercurrent carried by non-equlibrium quasi-particles in a multiterminal Josephson junction"*, Physical Review B 99, 075416 (2019).

Advances in the creation of hybrid nanostructures resulting from the pursuit in realization of topological quantum gates allowed to produce multi-terminal semiconductor nanostructures gated with superconducting electrodes. In the last work in this collection, we described a three-terminal Josephson junction defined on one-dimensional quantum wires contacted with superconductors. In such a system, when bias voltages are applied to the superconducting contacts, the transport properties are determined by multiple local and non-local Andreev reflections. To quantify the flow of current in such a structure, we extended the previously used approach **[H5]** such it allowed to describe multiple Andreev reflections in multimerminal systems.

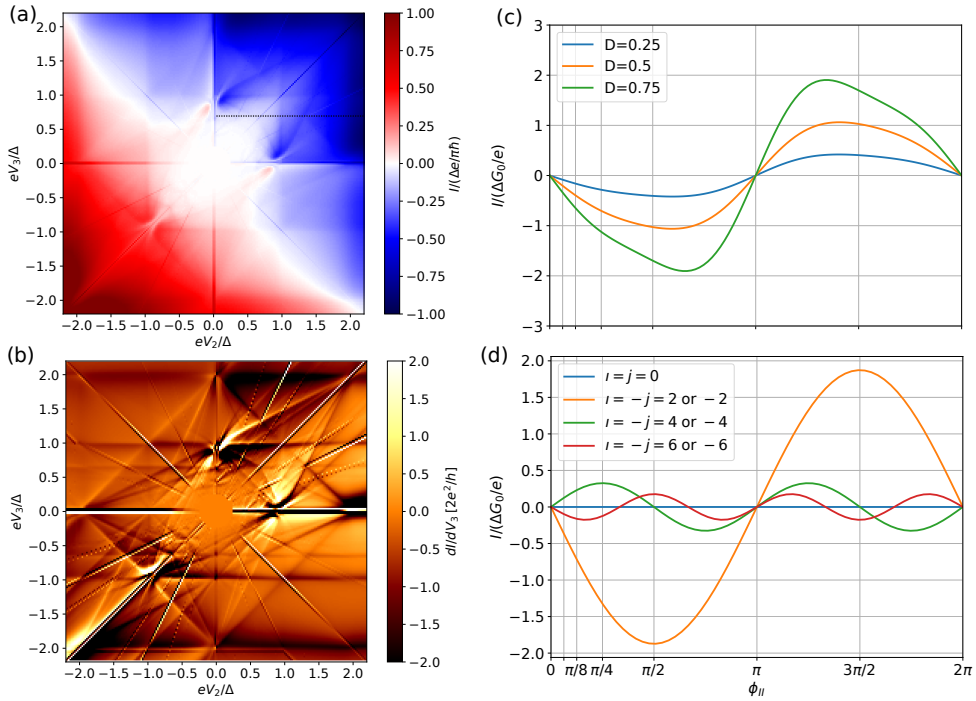

Figure 19: (a) The map of the current in the first contact of a three-terminal SNS junction under voltage bias on the superconducting contacts. (b) Differential conductance map. (c) Current between the second and third contact for equal voltages on these leads as a function of the phase of the pairing potential on the second contact. (d) Components of the supercurrent for a junction of intermediate transparency $D = 0.5$. **[H11]**.

We calculated the current in the first contact of the junction under the influence of voltages V_2 and V_3 [Fig. 19(a)], which was used to determine the differential conductance shown on the panel (b). The map clearly shows slanting lines intersecting the point $V_2 = V_3 = 0$ on the map. We showed that they result from a stepwise amplification of the current flowing through the leads when the voltages are commensurate with $iV_2 + jV_3 = 0$. This is caused by the appearance of additional DC current components, which for the noncommensurate voltages oscillate over time.

To analyze the nature of these components, we examined the current flowing between contacts to which the same voltage was applied. It turned out that the current between the second and third contact oscillates as the function of the phase of the pairing potential at the second contact [Fig. 19(b)]. Such a dependence of current on the superconducting phase with no voltage drop corresponds to the flow of supercurrent in the structure. In the system under consideration, however, this is surprising because the structure is by its nature dissipative, and the system has no bound states that typically carry superconducting current in two-terminal structures as considered in the paper **[H5]**. We have shown in our work that this current is induced by quasiparticles propagating from superconducting electrodes due to the non-local Andreev reflections. We showed that the critical value of this current depends on the junction transparency as $\sim D^n$ for the n'th component. Importantly, the current lines discussed in the work have been recently observed [50], and our work is the first theoretical analysis that could address this observation.

Summary

The works **[H1]** - **[H11]** present the results of theoretical and experimental-theoretical research on the properties of nanostructures in the presence of SO interaction and induced superconductivity. I consider the following as the most important results of these works:

- Indication of the effects of band mixing by SO interaction, which leads to spin polarization of the current flowing through the nanowire and allows for visualization of the presence of SO coupling by probing the way the current flows through a constriction in the channel.
- Demonstration of the presence of an extremely strong SO interaction in InSb nanowires leading to an observable helical gap.
- Theoretical interpretation of experimental results, which for the first time demonstrated the doubling of the conductance quantization of QPC nearby superconductor for structures realized both on 2DEG and nanowires, along with quantitative demonstration that conductance measurements of nanowires covered by a superconductor clearly show that the transport is ballistic.
- Explanation of the orbital effects on the formation of Majorana bound states along with an indication of the correct theoretical treatment the orbital effects of the magnetic field for hybrid nanostructures.
- Demonstration of a new type of superconducting current induced by quasiparticles in a multi-terminal Josephson junction.

These results have contributed to a better understanding of the properties of hybrid nanostructures, and the presented theoretical predictions may find applications in future studies of devices that allow to engineer topological phases.

Bibliography

[1] B. J. van Wees, H. van Houten, C. W. J. Beenakker, J. G. Williamson, L. P. Kouwenhoven, D. van der Marel, and C. T. Foxon, "Quantized conductance of point contacts in a two-dimensional electron gas," Phys. Rev. Lett. **60**, 848 (1988).

[2] S. Tarucha, D. G. Austing, T. Honda, R. J. van der Hage, and L. P. Kouwenhoven, "Shell Filling and Spin Effects in a Few Electron Quantum Dot," Phys. Rev. Lett. **77**, 3613–3616 (1996).

[3] S. Datta and B. Das, "Electronic analog of the electro-optic modulator," Appl. Phys. Lett. **56**, 665 (1990).

[4] D. Loss and D. P. DiVincenzo, "Quantum computation with quantum dots," Phys. Rev. A **57**, 120–126 (1998).

[5] K. C. Nowack, F. H. L. Koppens, Yu V. Nazarov, and L. M. K. Vandersypen, "Coherent Control of a Single Electron Spin with Electric Fields," Science **318**, 1430–1433 (2007).

[6] A. Yu Kitaev, "Unpaired Majorana fermions in quantum wires," Phys.-Usp. **44**, 131 (2001).

[7] R. M. Lutchyn, J. D. Sau, and S. Das Sarma, "Majorana Fermions and a Topological Phase Transition in Semiconductor-Superconductor Heterostructures," Phys. Rev. Lett. **105**, 077001 (2010).

[8] Y. Oreg, G. Refael, and F. von Oppen, "Helical Liquids and Majorana Bound States in Quantum Wires," Phys. Rev. Lett. **105**, 177002 (2010).

[9] G. Dresselhaus, "Spin-Orbit Coupling Effects in Zinc Blende Structures," Phys. Rev. **100**, 580 (1955).

[10] Yu A. Bychkov and E. I. Rashba, "Oscillatory effects and the magnetic susceptibility of carriers in inversion layers," J. Phys. C: Solid State Phys. **17**, 6039 (1984).

[11] V. Mourik, K. Zuo, S. M. Frolov, S. R. Plissard, E. P. a. M. Bakkers, and L. P. Kouwenhoven, "Signatures of Majorana Fermions in Hybrid Superconductor-Semiconductor Nanowire Devices," Science **336**, 1003 (2012).

[12] M. T. Deng, C. L. Yu, G. Y. Huang, M. Larsson, P. Caroff, and H. Q. Xu, "Anomalous Zero-Bias Conductance Peak in a Nb–InSb Nanowire–Nb Hybrid Device," Nano Lett. **12**, 6414–6419 (2012).

[13] A. D. K. Finck, D. J. Van Harlingen, P. K. Mohseni, K. Jung, and X. Li, "Anomalous Modulation of a Zero-Bias Peak in a Hybrid Nanowire-Superconductor Device," Phys. Rev. Lett. **110**, 126406 (2013).

[14] H. O. H. Churchill, V. Fatemi, K. Grove-Rasmussen, M. T. Deng, P. Caroff, H. Q. Xu, and C. M. Marcus, "Superconductor-nanowire devices from tunneling to the multichannel regime: Zero-bias oscillations and magnetoconductance crossover," Phys. Rev. B **87**, 241401 (2013).

[15] J. Chen, P. Yu, J. Stenger, M. Hocevar, D. Car, S. R. Plissard, E. P. A. M. Bakkers, T. D. Stanescu, and S. M. Frolov, "Experimental phase diagram of zero-bias conductance peaks in superconductor/semiconductor nanowire devices," Science Advances **3**, e1701476 (2017).

[16] D. Averin and A. Bardas, "ac Josephson Effect in a Single Quantum Channel," Phys. Rev. Lett. **75**, 1831 (1995).

[17] G. Schmidt, D. Ferrand, L. W. Molenkamp, A. T. Filip, and B. J. van Wees, "Fundamental obstacle for electrical spin injection from a ferromagnetic metal into a diffusive semiconductor," Phys. Rev. B **62**, R4790 (2000).

[18] B. Szafran, "Scanning gate microscopy simulations for quantum rings: Effective potential of the tip and conductance maps," Phys. Rev. B **84**, 075336 (2011).

[19] M. A. Topinka, B. J. LeRoy, S. E. J. Shaw, E. J. Heller, R. M. Westervelt, K. D. Maranowski, and A. C. Gossard, "Imaging Coherent Electron Flow from a Quantum Point Contact," Science **289**, 2323–2326 (2000).

[20] V. N. Golovach, M. Borhani, and D. Loss, "Electric-dipole-induced spin resonance in quantum dots," Phys. Rev. B **74**, 165319 (2006).

[21] K. D. Petersson, L. W. McFaul, M. D. Schroer, M. Jung, J. M. Taylor, A. A. Houck, and J. R. Petta, "Circuit quantum electrodynamics with a spin qubit," Nature **490**, 380 (2012).

[22] J. Stehlik, M. D. Schroer, M. Z. Maialle, M. H. Degani, and J. R. Petta, "Extreme Harmonic Generation in Electrically Driven Spin Resonance," Phys. Rev. Lett. **112**, 227601 (2014).

[23] C. W. J. Beenakker, "Quantum transport in semiconductor-superconductor microjunctions," Phys. Rev. B **46**, 12841 (1992).

[24] T. Ando, "Quantum point contacts in magnetic fields," Phys. Rev. B **44**, 8017 (1991).

[25] Y.-J. Doh, J. A. van Dam, A. L. Roest, E. P. A. M. Bakkers, L. P. Kouwenhoven, and S. De Franceschi, "Tunable Supercurrent Through Semiconductor Nanowires," Science **309**, 272 (2005).

[26] Jie Xiang, A. Vidan, M. Tinkham, R. M. Westervelt, and Charles M. Lieber, "Ge/Si nanowire mesoscopic Josephson junctions," Nature Nanotechnology **1**, 208 (2006).

[27] S. Li, N. Kang, D. X. Fan, L. B. Wang, Y. Q. Huang, P. Caroff, and H. Q. Xu, "Coherent Charge Transport in Ballistic InSb Nanowire Josephson Junctions," Scientific Reports **6**, 24822 (2016).

[28] A. Chrestin, T. Matsuyama, and U. Merkt, "Evidence for a proximity-induced energy gap in Nb/InAs/Nb junctions," Phys. Rev. B **55**, 8457 (1997).

[29] H. J. Suominen, M. Kjaergaard, A. R. Hamilton, J. Shabani, C. J. Palmstrøm, C. M. Marcus, and F. Nichele, "Zero-Energy Modes from Coalescing Andreev States in a Two-Dimensional Semiconductor-Superconductor Hybrid Platform," Phys. Rev. Lett. **119**, 176805 (2017).

[30] E. C. T. O'Farrell, A. C. C. Drachmann, M. Hell, A. Fornieri, A. M. Whiticar, E. B. Hansen, S. Gronin, G. C. Gardner, C. Thomas, M. J. Manfra, K. Flensberg, C. M. Marcus, and F. Nichele, "Hybridization of Subgap States in One-Dimensional Superconductor-Semiconductor Coulomb Islands," Phys. Rev. Lett. **121**, 256803 (2018).

[31] C. G. L. Bøttcher, F. Nichele, M. Kjaergaard, H. J. Suominen, J. Shabani, C. J. Palmstrøm, and C. M. Marcus, "Superconducting, insulating and anomalous metallic regimes in a gated two-dimensional semiconductor–superconductor array," Nature Physics **14**, 1138 (2018).

[32] A. Fornieri, A. M. Whiticar, F. Setiawan, E. P. Marín, A. C. C. Drachmann, A. Keselman, S. Gronin, C. Thomas, T. Wang, R. Kallaher, G. C. Gardner, E. Berg, M. J. Manfra, A. Stern, C. M. Marcus, and F. Nichele, "Evidence of topological superconductivity in planar Josephson junctions," arXiv:1809.03037 (2018).

[33] A. Pfund, I. Shorubalko, K. Ensslin, and R. Leturcq, "Spin-state mixing in InAs double quantum dots," Phys. Rev. B **76**, 161308 (2007).

[34] C. Fasth, A. Fuhrer, L. Samuelson, Vitaly N. Golovach, and Daniel Loss, "Direct Measurement of the Spin-Orbit Interaction in a Two-Electron InAs Nanowire Quantum Dot," Phys. Rev. Lett. **98**, 266801 (2007).

[35] H. A. Nilsson, P. Caroff, C. Thelander, M. Larsson, J. B. Wagner, L.-E. Wernersson, L. Samuelson, and H. Q. Xu, "Giant, Level-Dependent g Factors in InSb Nanowire Quantum Dots," Nano Lett. **9**, 3151 (2009).

[36] J. Liu, A. C. Potter, K. T. Law, and P. A. Lee, "Zero-Bias Peaks in the Tunneling Conductance of Spin-Orbit-Coupled Superconducting Wires with and without Majorana End-States," Phys. Rev. Lett. **109**, 267002 (2012).

[37] D. I. Pikulin, J. P. Dahlhaus, M. Wimmer, H. Schomerus, and C. W. J. Beenakker, "A zero-voltage conductance peak from weak antilocalization in a Majorana nanowire," New J. Phys. **14**, 125011 (2012).

[38] D. Bagrets and A. Altland, "Class D Spectral Peak in Majorana Quantum Wires," Phys. Rev. Lett. **109**, 227005 (2012).

[39] J. Alicea, Y. Oreg, G. Refael, F. von Oppen, and M. P. A. Fisher, "Non-Abelian statistics and topological quantum information processing in 1d wire networks," Nature Physics **7**, 412 (2011).

[40] B. van Heck, A. R. Akhmerov, F. Hassler, M. Burrello, and C. W. J. Beenakker, "Coulomb-assisted braiding of Majorana fermions in a Josephson junction array," New J. Phys. **14**, 035019 (2012).

[41] T. Hyart, B. van Heck, I. C. Fulga, M. Burrello, A. R. Akhmerov, and C. W. J. Beenakker, "Flux-controlled quantum computation with Majorana fermions," Phys. Rev. B **88**, 035121 (2013).

[42] S. R. Plissard, I. van Weperen, D. Car, M. A. Verheijen, G. W. G. Immink, Jakob Kammhuber, Ludo J. Cornelissen, Daniel B. Szombati, Attila Geresdi, Sergey M. Frolov, Leo P. Kouwenhoven, and Erik P. A. M. Bakkers, "Formation and electronic properties of InSb nanocrosses," Nature Nanotechnology **8**, 859 (2013).

[43] E. M. T. Fadaly, H. Zhang, S. Conesa-Boj, D. Car, Ö. Gül, S. R. Plissard, R. L. M. Op het Veld, S. Kölling, L. P. Kouwenhoven, and E. P. A. M. Bakkers, "Observation of Conductance Quantization in InSb Nanowire Networks," Nano Lett. **17**, 6511 (2017).

[44] S. Gazibegovic, D. Car, H. Zhang, S. C. Balk, J. A. Logan, M. W. A. de Moor, M. C. Cassidy, R. Schmits, D. Xu, G. Wang, P. Krogstrup, R. L. M. Op het Veld, K. Zuo, Y. Vos, J. Shen, D. Bouman, B. Shojaei, D. Pennachio, J. S. Lee, P. J. van Veldhoven, S. Koelling, M. A. Verheijen, L. P. Kouwenhoven, C. J. Palmstrøm, and E. P. A. M. Bakkers, "Epitaxy of advanced nanowire quantum devices," Nature **548**, 434 (2017).

[45] O. Dmytruk and J. Klinovaja, "Suppression of the overlap between Majorana fermions by orbital magnetic effects in semiconducting-superconducting nanowires," Phys. Rev. B **97**, 155409 (2018).

[46] J. S. Lim, L. Serra, R. López, and R. Aguado, "Magnetic-field instability of Majorana modes in multiband semiconductor wires," Phys. Rev. B **86**, 121103 (2012).

[47] J. Osca and L. Serra, "Majorana states and magnetic orbital motion in planar hybrid nanowires," Phys. Rev. B **91**, 235417 (2015).

[48] B. Nijholt and A. R. Akhmerov, "Orbital effect of magnetic field on the Majorana phase diagram," Phys. Rev. B **93**, 235434 (2016).

[49] S. M. Albrecht, A. P. Higginbotham, M. Madsen, F. Kuemmeth, T. S. Jespersen, J. Nygård, P. Krogstrup, and C. M. Marcus, "Exponential protection of zero modes in Majorana islands," Nature **531**, 206 (2016).

[50] Y. Cohen, Y. Ronen, J.-H. Kang, M. Heiblum, D. Feinberg, R. Mélin, and H. Shtrikman, "Non-local supercurrent of quartets in a three-terminal Josephson junction," PNAS **115**, 6991–6994 (2018).

5. Description of other scientific achievements

My other research achievements can be divided into two categories: (i) works done before obtaining the doctoral degree, in which I mainly focused on the description of the effects of SO in artificial atoms and molecules, and (ii) the works resulting from post-doctoral research, in which I expanded my interests also to: description of hole states and exciton quantum dots, electron transport in superconducting structures. Below I will briefly discuss only selected, most important results.

5.1. Works realized before obtaining Ph. D. degree

[P1] **M. P. Nowak**, B. Szafran, F. M. Peeters, *"Manipulation of two-electron states by the electric field in stacked self-assembled dots"*, J. Phys.: Condens. Matter 20, 395225 (2008).

[P2] B. Szafran, **M. P. Nowak**, S. Bednarek, T. Chwiej, and F. M. Peeters, *"Selective suppression of Dresselhaus or Rashba spin-orbit coupling effects by the Zeeman interaction in quantum dots"*, Phys. Rev. B 79, 235303 (2009).

[P3] **M. P. Nowak** and B. Szafran, *"Spin-orbit coupling effects in two-dimensional circular quantum rings: Elliptical deformation of confined electron density"*, Phys. Rev. B 80, 195319 (2009).

[P4] **M. P. Nowak** and B. Szafran, *"Coupling of bonding and antibonding electron orbitals in double quantum dots by spin-orbit interaction"*, Phys. Rev. B 81, 235311 (2010).

[P5] **M. P. Nowak** and B. Szafran, *"Time-dependent configuration-interaction simulations of spin swap in spin-orbit-coupled double quantum dots"*, Phys. Rev. B 82, 165316 (2010).

[P6] **M. P. Nowak** and B. Szafran, *"Singlet-triplet avoided crossings and effective g factor versus spatial orientation of spin-orbit-coupled quantum dots"*, Phys. Rev. B 83, 035315 (2011).

[P7] **M. P. Nowak**, B. Szafran, F. M. Peeters, B. Partoens, and W. J. Pasek, *"Tuning of the spin-orbit interaction in a quantum dot by an in-plane magnetic field"*, Phys. Rev. B 83, 245324 (2011).

[P8] **M. P. Nowak**, B. Szafran, and F. M. Peeters, *"Fano resonances and electron spin transport through a two-dimensional spin-orbit-coupled quantum ring"*, Phys. Rev. B 84, 235319 (2011).

[P9] **M. P. Nowak**, B. Szafran, and F. M. Peeters, *"Resonant harmonic generation and collective spin rotations in electrically driven quantum dots"*, Phys. Rev. B 86, 125428 (2012).

[P10] **M. P. Nowak** and B. Szafran, *"Spin-polarization anisotropy in a narrow spin-orbit-coupled nanowire quantum dot"*, Phys. Rev. B 87, 205436 (2013).

The subject of my doctorate concerned the electronic structure of artificial atoms and molecules under the influence of SO interaction. This topic was then intensively explored by numerous groups in the world due to the opening prospects of the construction of a quantum computer, whose elements would base on the electrical control over the electron spin. During the doctoral studies we were able to describe in a numerically exact way multi-electron quantum rings with finite channel width and explain the effects of breaking the symmetry of spatial distribution of the charge by SO interaction [P3]. We described the spin polarization anisotropy, which manifests itself in the repulsion of energy levels of artificial atoms [P4] [P6]. What is most important we provided the explanation of experiments that measured the electronic structure of self-organized quantum dots [P7] and electric excitation of charge

carrier spins [P9]. The theory proposed by us was then used by other researchers to interpret following experimental measurements. During my Ph. D. I conducted research at the AGH University of Science and Technology and at the University of Antwerp, which allowed me to obtain doctoral degrees from both the universities. The works [P1]-[P10] became the foundation for my following research, where the subject of multi-electron quantum dots in nanowires evolved towards hybrid structures – covered with superconductor – which at the time when I finished my Ph. D. were investigated for the first time.

5.2. Works realized after Ph. D.

[P11] E. N. Osika, B. Szafran, and **M. P. Nowak**, *"Simulations of electric-dipole spin resonance for spin-orbit coupled quantum dots in the Overhauser field: Fractional resonances and selection rules"*, Phys. Rev. B 88, 165302 (2013).

[P12] W. J. Pasek, **M. P. Nowak**, B. Szafran, *"Optical signatures of valence-band mixing in positive trion recombination spectra of double quantum dots"*, Phys. Rev. B 89, 245303 (2014).

[P13] W. J. Pasek, **M. P. Nowak**, B. Szafran, *"Spin exchange energy for a pair of valence band holes in artificial molecules"*, Semicond. Sci. Technol. 29, 115022 (2014).

[P14] **M. P. Nowak** B. Szafran, *"Spontaneous and resonant lifting of the spin blockade in nanowire quantum dots"*, Phys. Rev. B 89, 205412 (2014).

[P15] W. J. Pasek, **M. P. Nowak** B. Szafran, *"Valence band mixing versus higher harmonic generation in electric-dipole spin resonance"*, Semicond. Sci. Technol. 30, 055017 (2015).

[P16] R. Ferdous, E. Kawakami, P. Scarlino, **M. P. Nowak**, D. R. Ward, D. E. Savage, M. G. Lagally, S. N. Coppersmith, M. Friesen, M. A. Eriksson, L. M. K. Vandersypen, R. Rahman, *"Valley dependent anisotropic spin splitting in silicon quantum dots"*, npj Quantum Information 4, 26 (2018).

The above works focused on the theoretical description of electron, hole and exciton states of semiconductor quantum dots. We showed, among other things, that resonant spin rotation can be carried out in the hyperfine field that stems nanowire atomic nuclei [P11] and that Pauli blockade is lifted spontaneously by the deexcitation of the triplet state mediated by phonons [P14] in agreement with the experiment. As part of cooperation with the experimental group of Prof. Lieven Vandersypen from the Technical University of Delft I analyzed, so far neglected, effects of SO interaction in silicon quantum dots [P16].

[P17] K. Kolasiński, B. Szafran, **M. P. Nowak**, *"Imaging of double slit interference by scanning gate microscopy"*, Phys. Rev. B 90, 165303 (2014).

[P18] B. Szafran, **M. P. Nowak**, E. Wach, D. P. Żebrowski, *"Interaction effects near constriction of a quasi two-dimensional electron system: an exact diagonalization study"*, Phys. Lett. A 378, 1036 (2014).

These works investigated electron transport in 2DEG. Particularly noteworthy is the work [P18], where the exact multi-electron calculations showed that in QPC the electron-electron interaction results in the formation of a spin polarized charge island – responsible for the experimentally observed anomalous conductance plateau – a hypothesis that has been the subject of ongoing debate and was verified previously only with methods treating the interaction in an approximate way.

[P19] H. Zhang, Ö. Gül, S. Conesa-Boj, K. Zuo, V. Mourik, F. K. de Vries, J. van Veen, D. J. van Woerkom, **M. P. Nowak**, M. Wimmer, D. Car, S. Plissard, E. P. A. M. Bakkers, M. Quintero-Pérez, S. Goswami, K. Watanabe, T. Taniguchi, L. P. Kouwenhoven, *"Ballistic Majorana nanowire devices"*, arXiv:1603.04069v1 (2016).

[P20] Ö. Gül, H. Zhang, F. K. de Vries, J. van Veen, K. Zuo, V. Mourik, S. Conesa-Boj, **M. P. Nowak**, D. J. van Woerkom, M. Quintero-Pérez, M. C. Cassidy, A. Geresdi, S. Kölling, D. Car, S. R. Plissard, E. P. A. M. Bakkers, L. P. Kouwenhoven, *"Hard superconducting gap in InSb nanowires"*, Nano. Lett., 17, 2690 (2017).

[P21] F. K. de Vries, J. Shen, R. J. Skolasinski, **M. P. Nowak**, D. Varjas, L. Wang, M. Wimmer, J. Ridderbos, F. A. Zwanenburg, A. Li, S. Koelling, M. A. Verheijen, E. P. A. M. Bakkers, L. P. Kouwenhoven, 2018, *"Spin-orbit interaction and induced superconductivity in an one-dimensional hole gas"*, Nano Lett. 18, 6483 (2018).

In the works [P20]-[P21] I theoretically analyzed the electrically tuned Josephson junctions created in semiconductor nanowires. We demonstrated how multiple Andreev reflections can be used to estimate the transparency of the junction, the number of subbands and the induced superconducting gap in the semiconductor. We have shown that the nanowire junctions implmented experimentally are transparent, and that the current is carried only by one [P20] subband of transverse quantization. This information is important in the context of ongoing work on the measurement of Majorana fermions using the *Photon Assisted Tunneling* method, where the number of propagating modes in the structure is key to the interpretation of the measurement. By analyzing the multiple Andreev reflections, we also demonstrated that the newly produced semiconductor nanowires allow the creation of a one-dimensional hole gas that can be used in a new generation of hybrid nanostructures [P21].

5.3. Bibliometric record of all the publications

Total number of publications: 32, in the Web of Science database: 31
Number of citations: 395, without self-citations: 346.
Index H: 11